Applications of active targets

A brief tour of experimental results

D. Bazin
National Superconducting Cyclotron Laboratory
Facility for Rare Isotope Beams
Michigan State University

Early days: Maya

- First electronic active target
- Use proven technologies
- Wires for electron amplification
- Conventional electronics
- Si-CsI ancillary detectors
- Gas volume not large enough to stop most charged particles

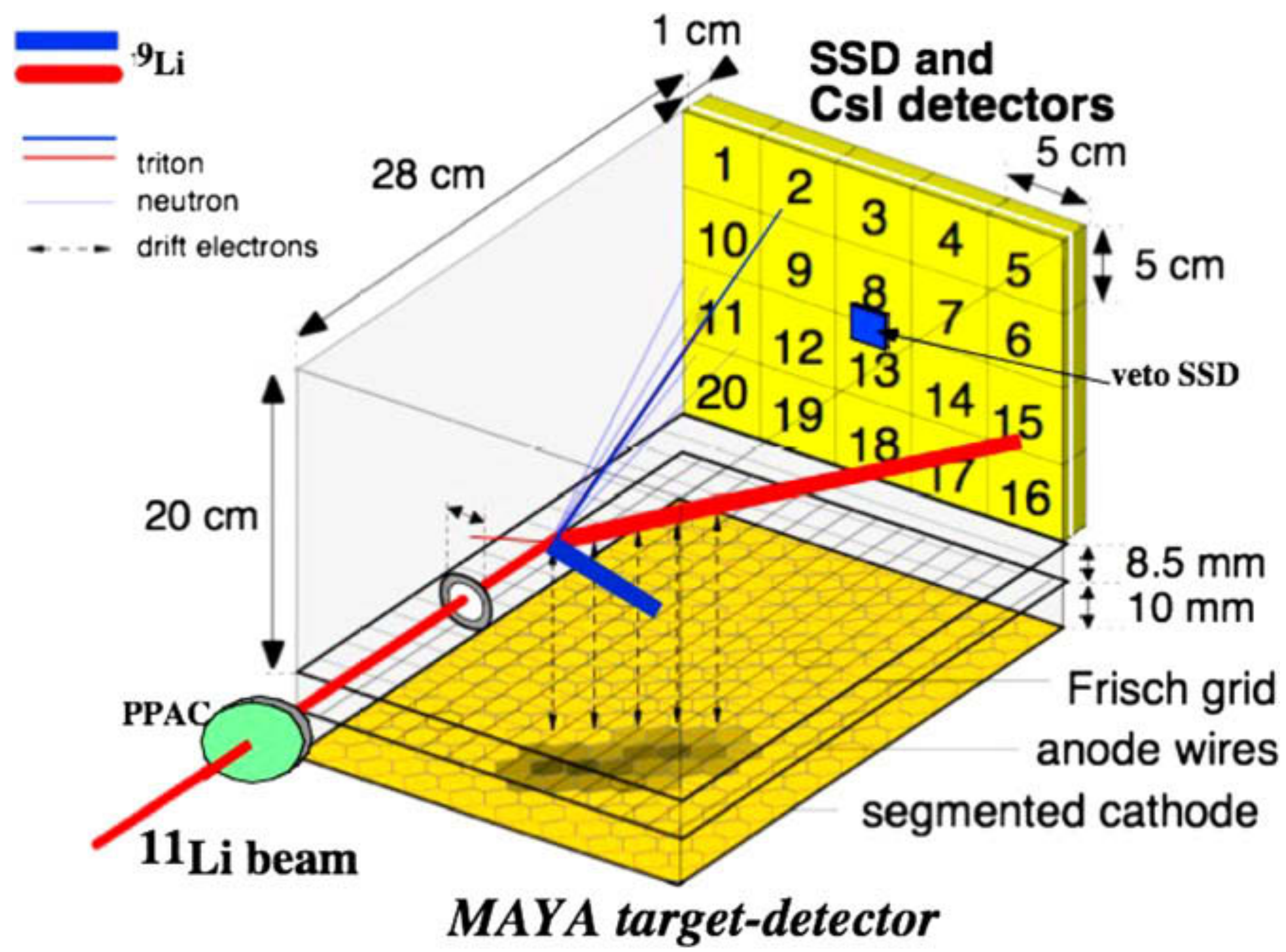

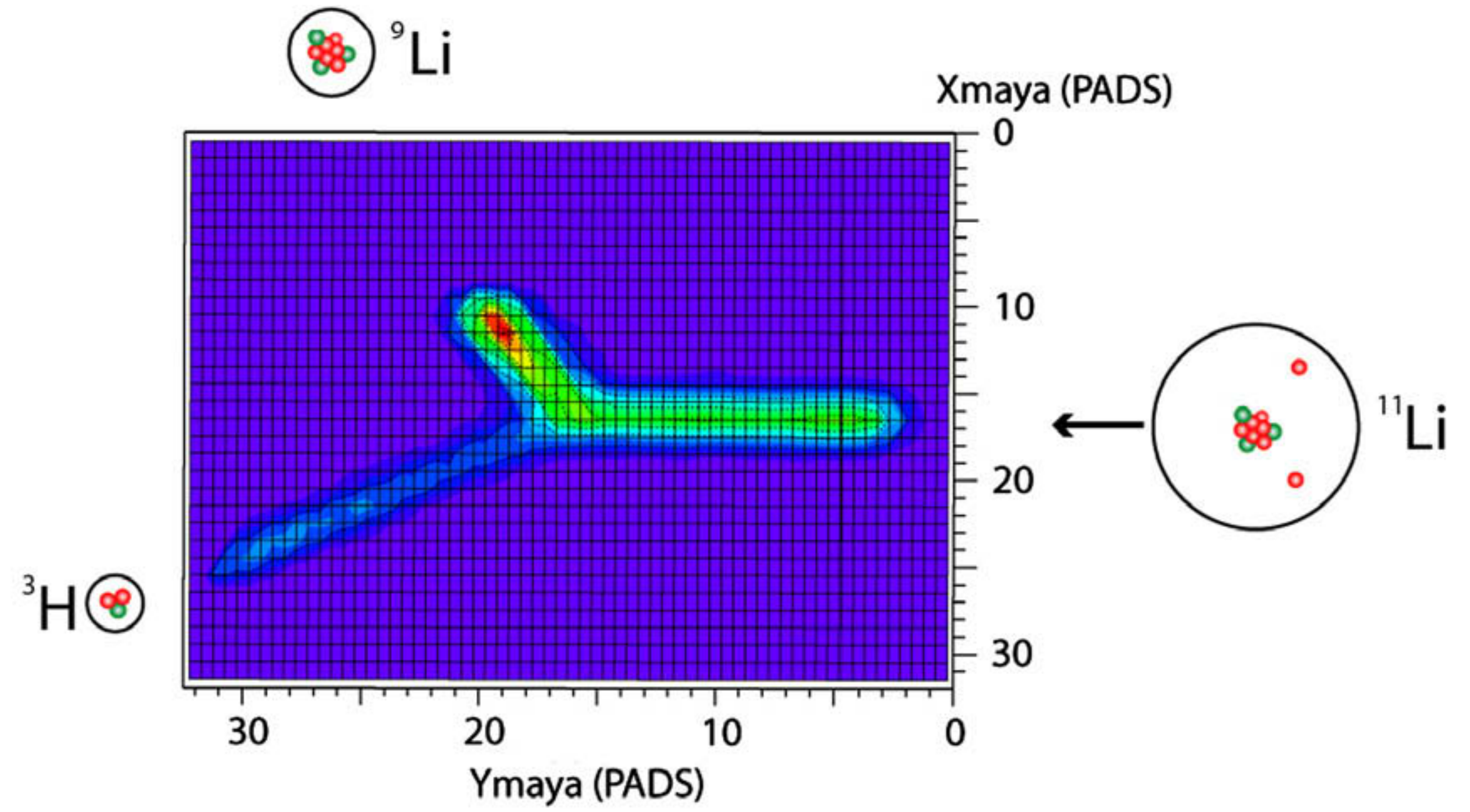

H. Savajols et al., NIM B 266 (2008) 4583–4588

Maya: results

- ^{11}Li(p,t)^{9}Li reaction at 3.6 MeV/u
- Energy-range and scattering angle correlations between the recoil ^{9}Li and scattered triton
- Events corresponding to the population of the first excited state ($1/2^-$) in ^{9}Li are clearly separated
- Mass of ^{11}Li can be deduced from Q-value measurement and known masses of ^{9}Li and triton

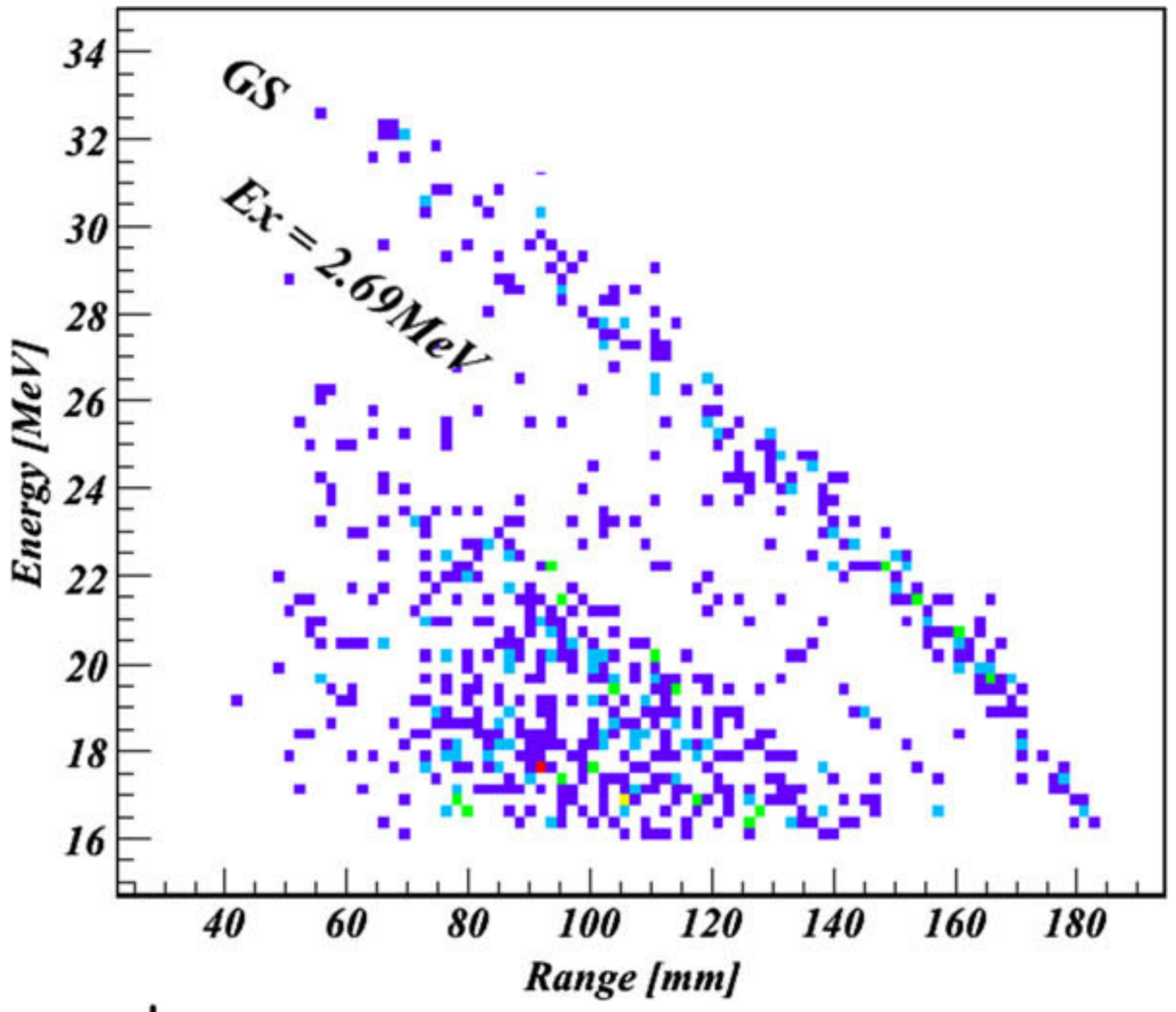

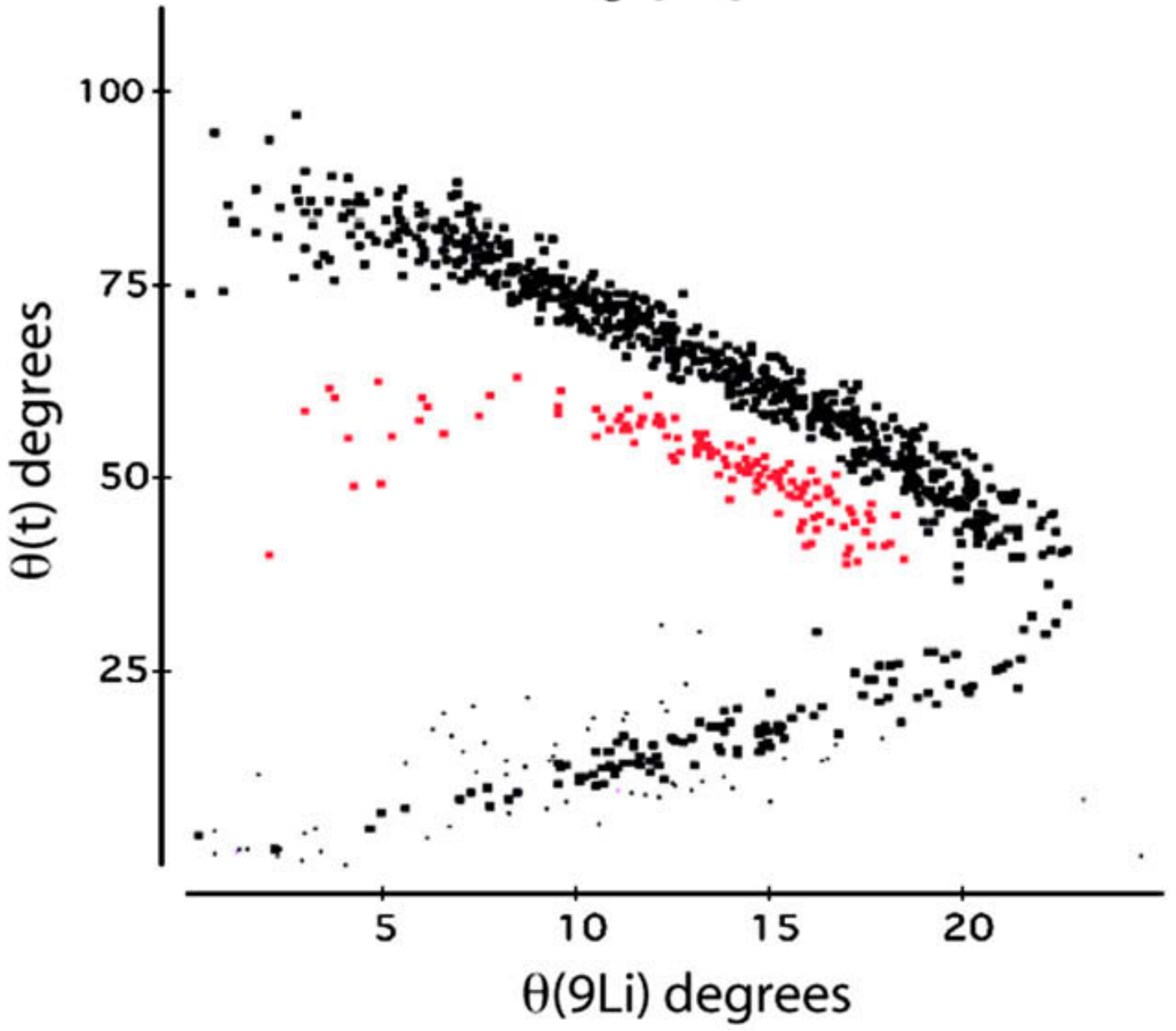

Maya: results

- Particle identification from Si-CsI telescopes or charge deposited in gas vs Si for heavier particles
- Measured angular distribution of the (p,t) reaction for gs and 1st excited state in ^{9}Li
- Data clearly favors P3 model, in which WF has *p* and *s* orbital mixing including 3-body correlations

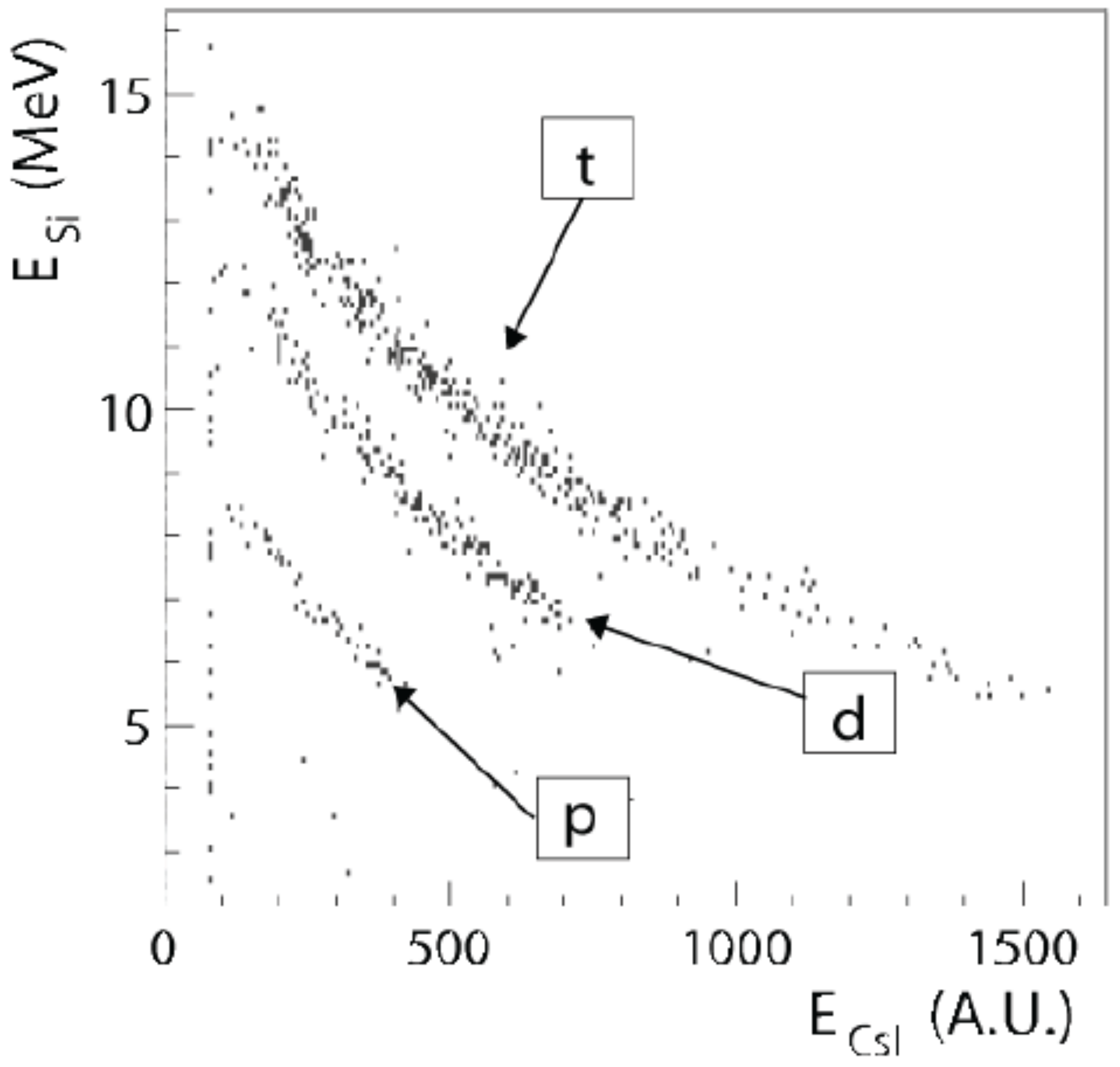

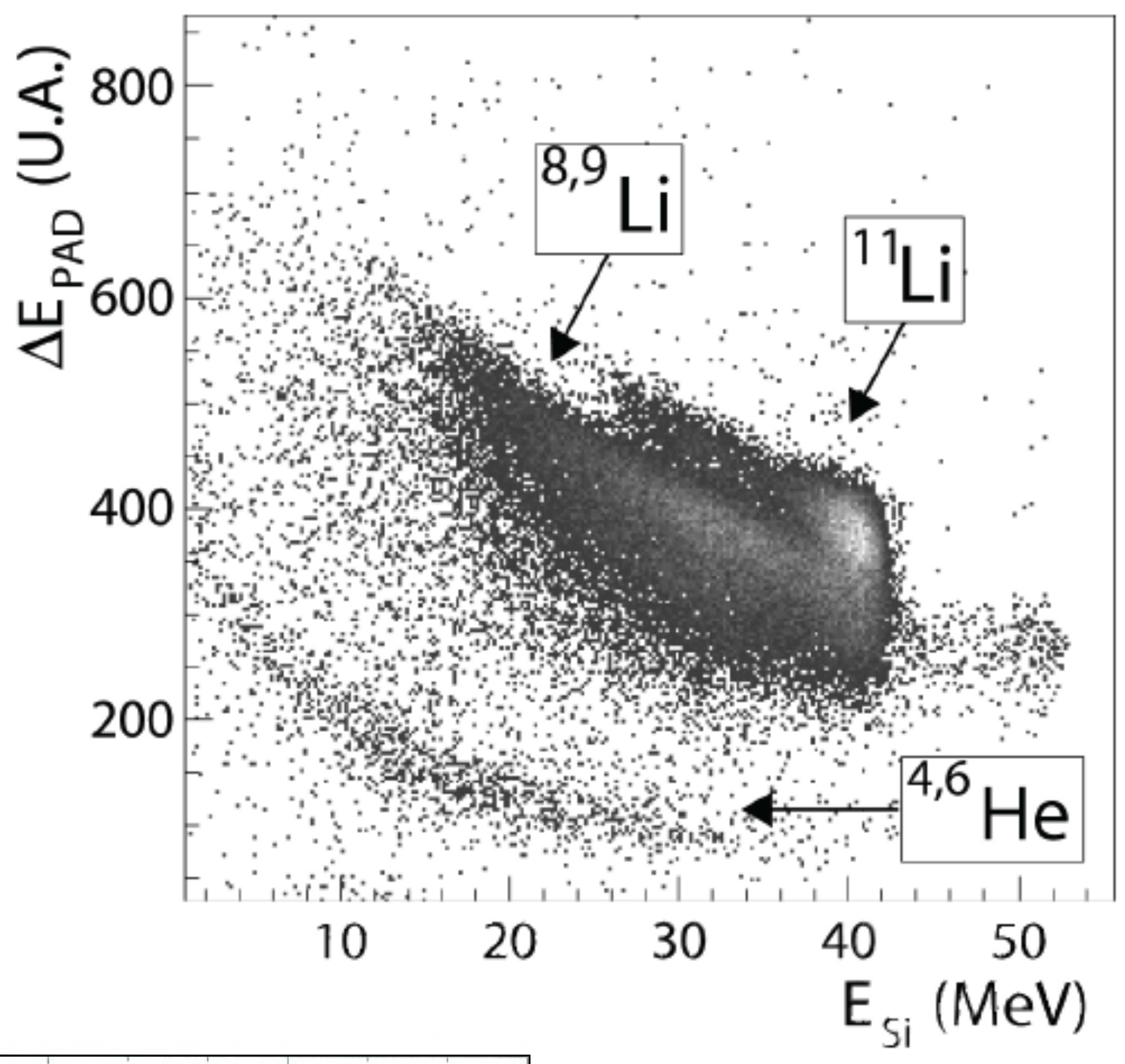

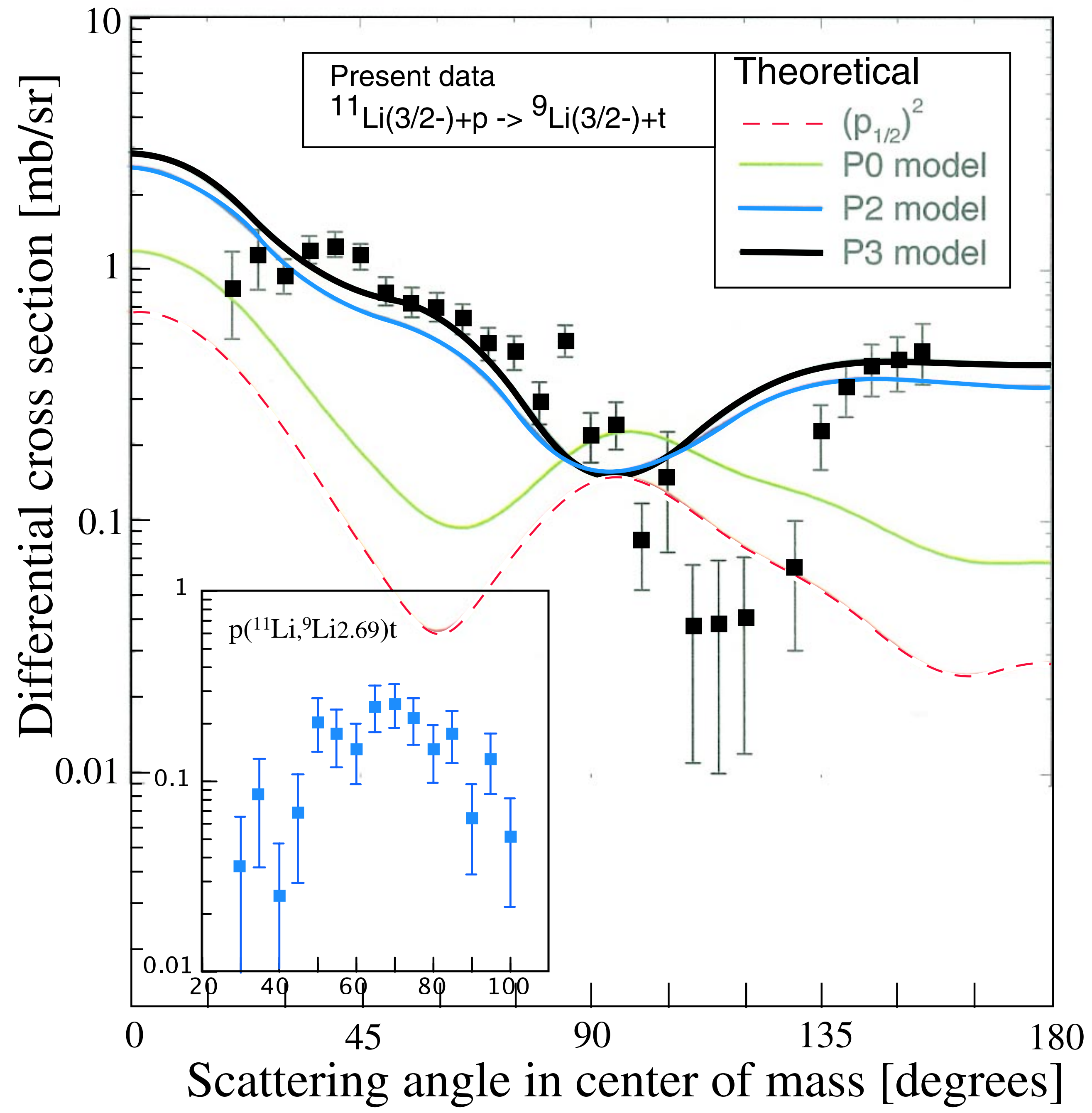

I. Tanihata et al., PRL 100, 192502 (2008)

IKAR: proton scattering at high energy

- Proton elastic scattering at ~ 1 GeV/u
  - Sensitive to nuclear matter density
  - Requires detection of scattered proton
- IKAR active target detector
  - Active target volume filled with 10 bar H_2
  - 6 detector cells in vessel
  - Each cell provide vertex position of reaction and scattering angle of proton

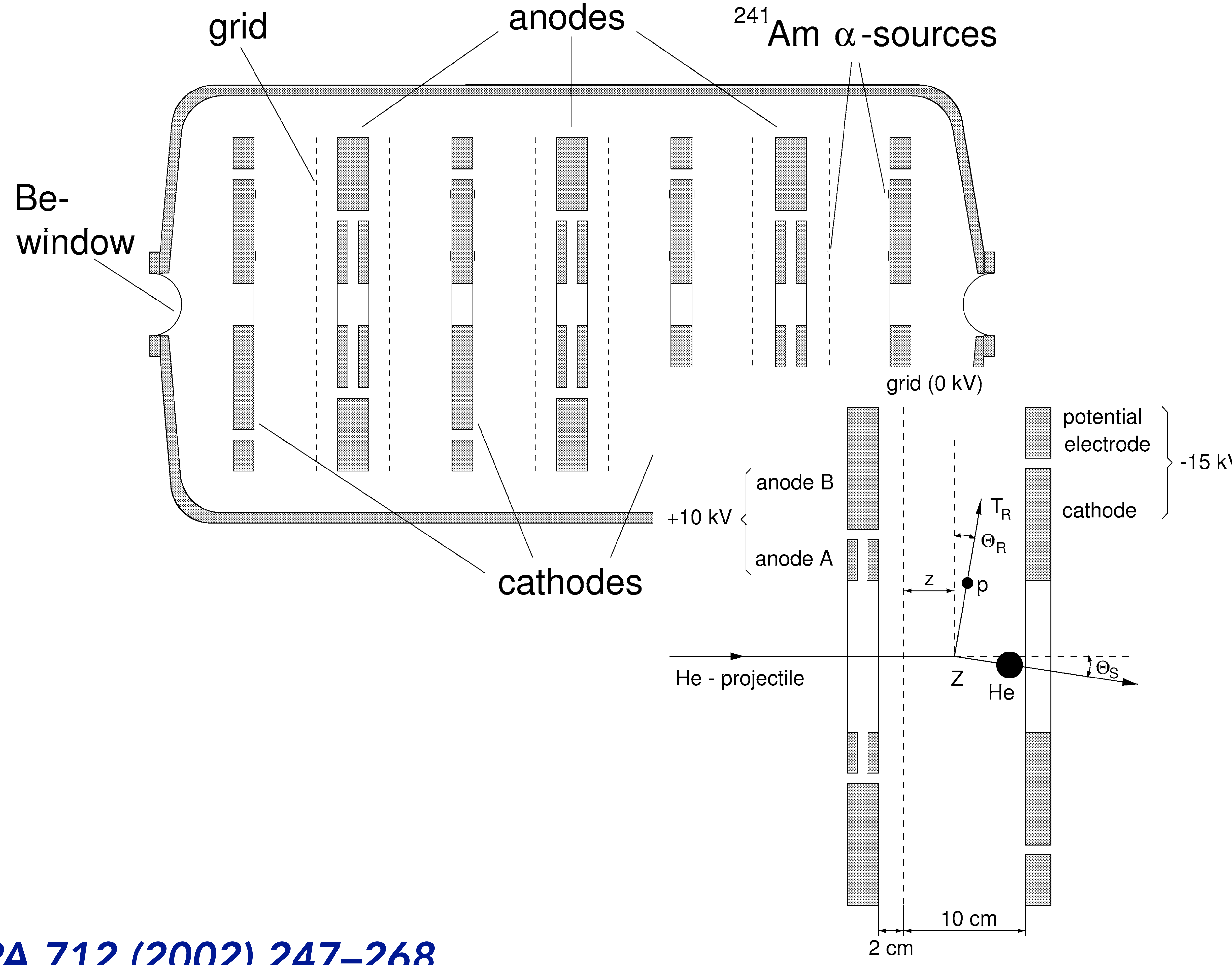

S.R. Neumaier et al., NPA 712 (2002) 247–268

IKAR: results

- Halo structure of He neutron-rich isotopes
- ^{4,6,8}He beams at ~ 0.7 GeV/u
- Differential cross sections measured vs momentum transfer
- Slopes at high momentum transfer are clearly different
- Comparison with matter density models

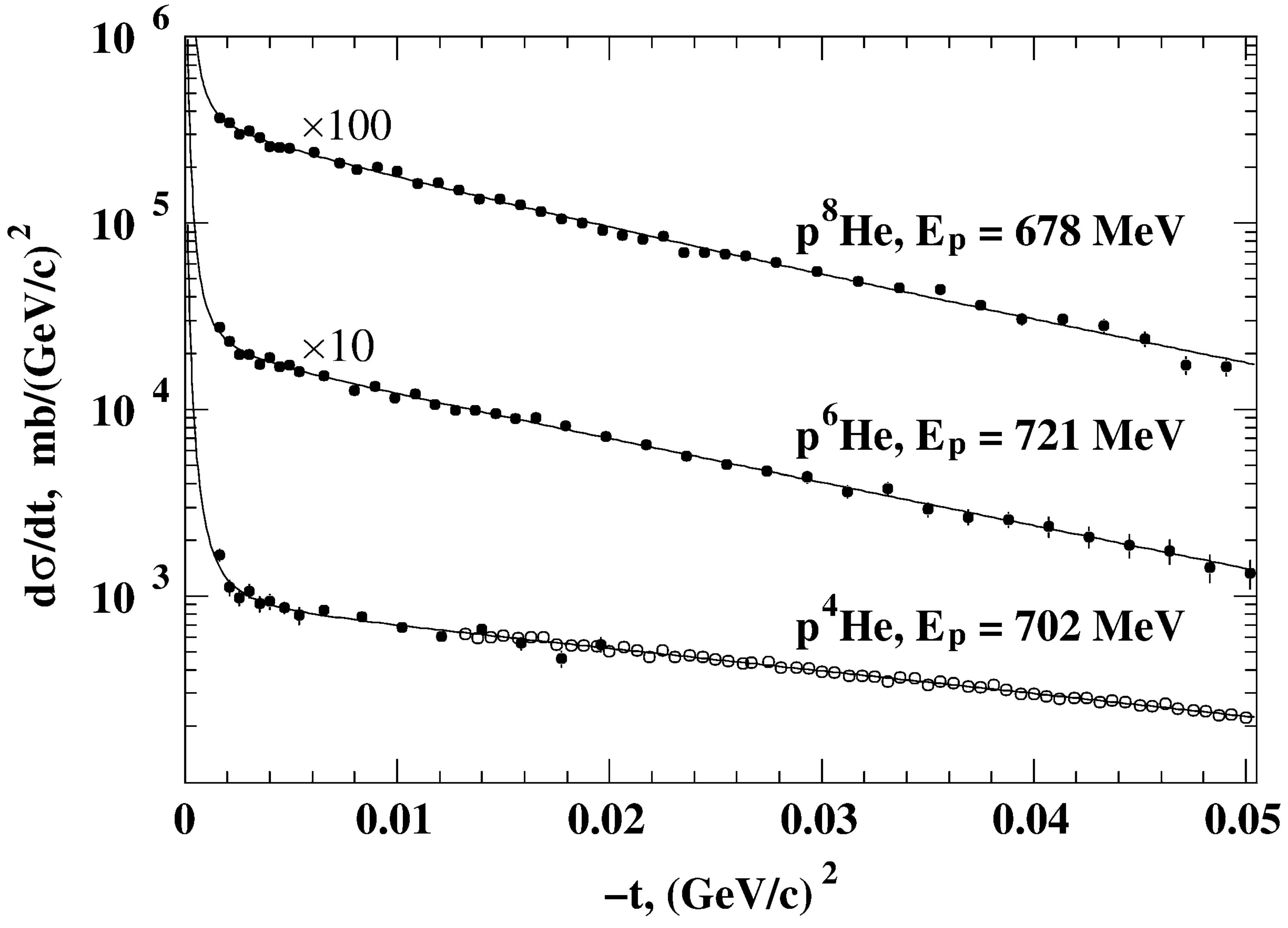

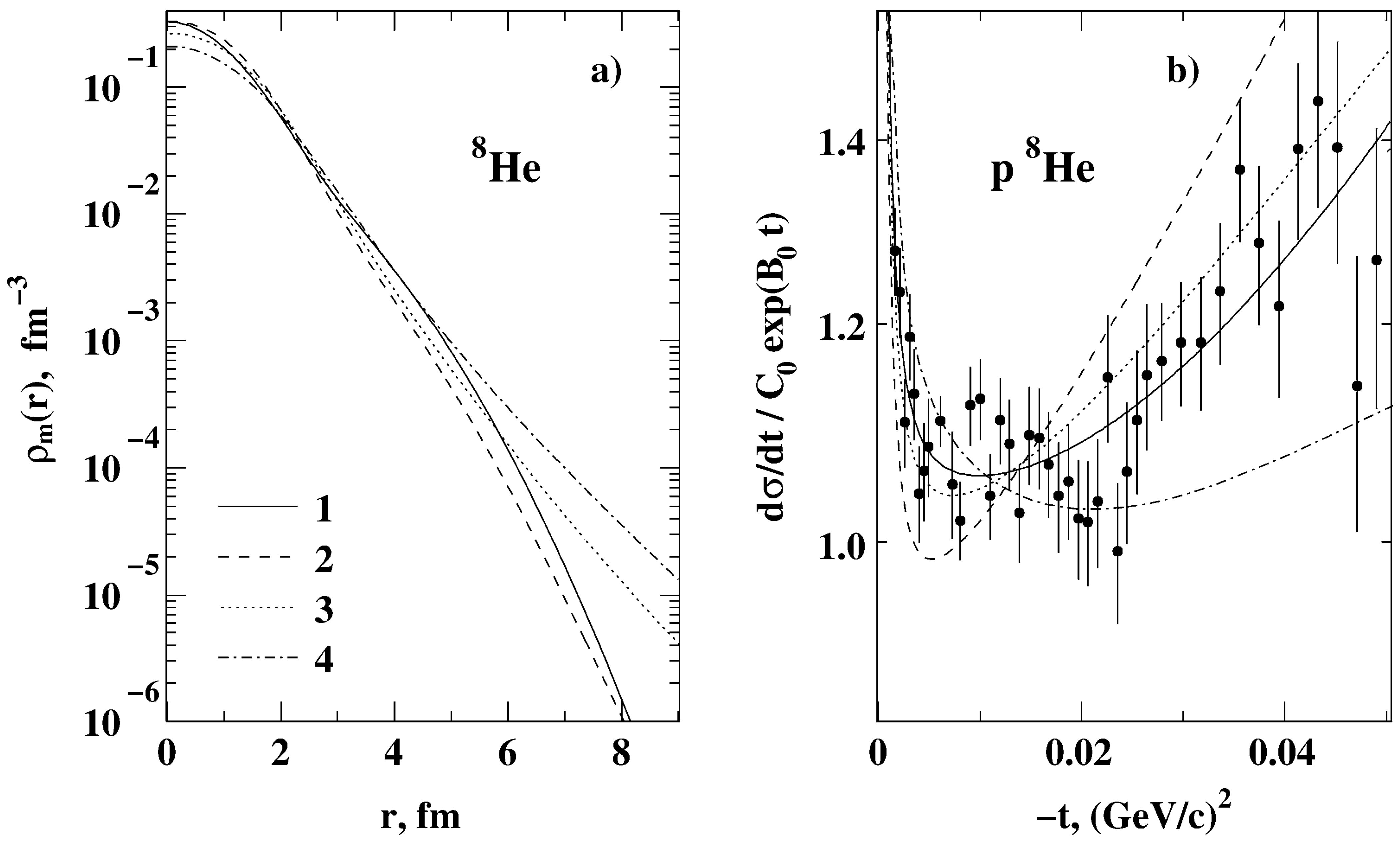

G.D. Alkhazov et al. / NPA 712 (2002) 269–299

MUSIC active target

- Energy loss profile detector
- Clever anode structure design
- Focus on detecting residue (beam-like particle) rather than recoil
- Very well adapted to fusion reactions
- Small number of electronics channels
- Small electron drift distance reduces detector dead time
- Can accepts higher beam intensities than Time Projection Chambers

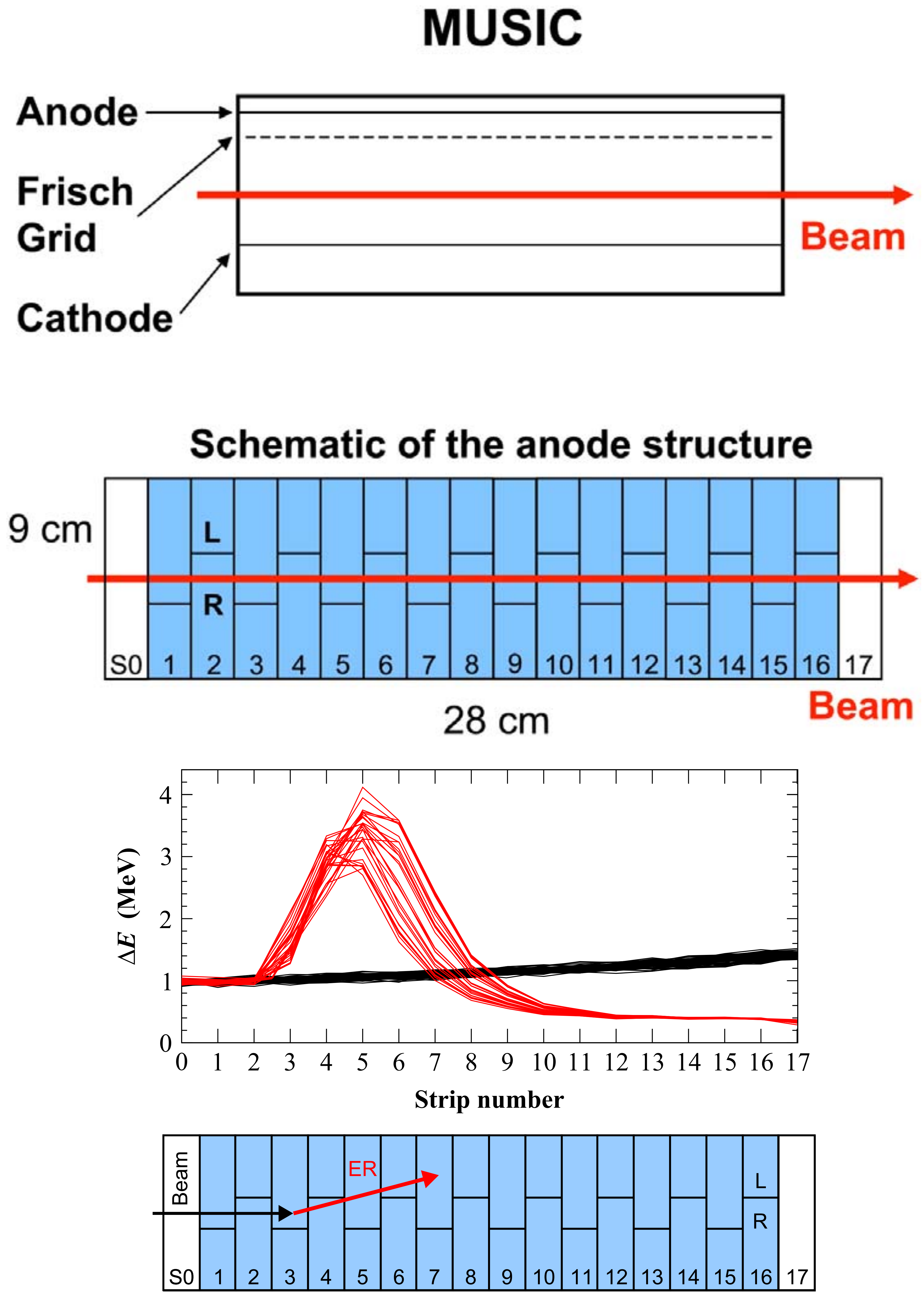

P.F.F. Carnelli NIM A 799 (2015) 197–202

MUSIC active target: results

- Reaction channel identification
- ^{23}Na beam on ^{4}He target
- Relative energy loss between adjacent strips
- (α,n) and (α,p) clearly resolved from elastic and inelastic scattering
- Excitation functions of all reactions measured simultaneously

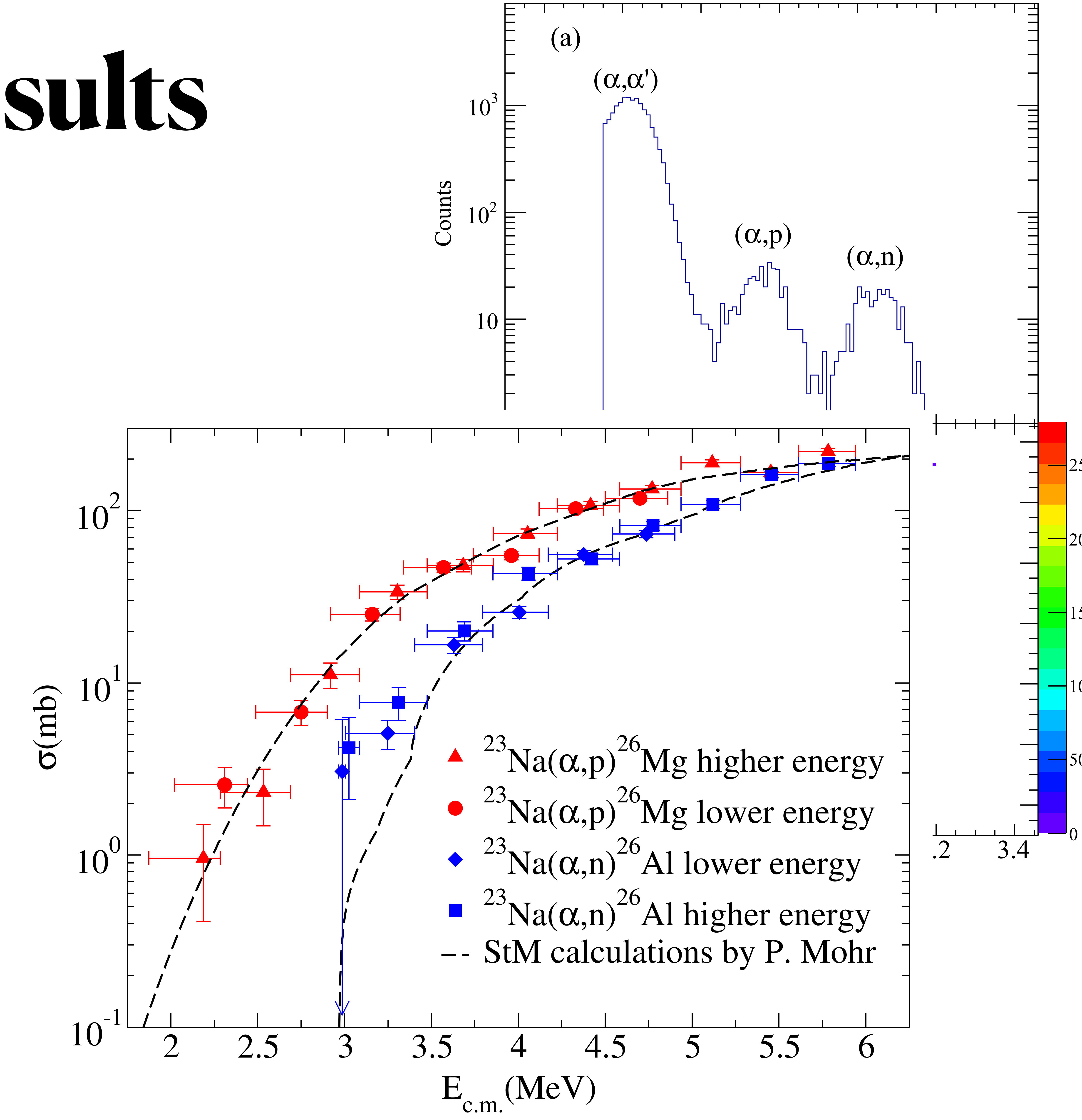

M.L. Avila NIM A 859 (2017) 63–68

Maiko

- Similar geometry as ACTAR
- Using microPIC technology for electron amplification
- Inelastic scattering $^{12}C(\alpha,\alpha')^{12}C^*$ to populate Hoyle state (3α state) in ^{12}C
- Clear identification of ^{12}C decay into 3α particles

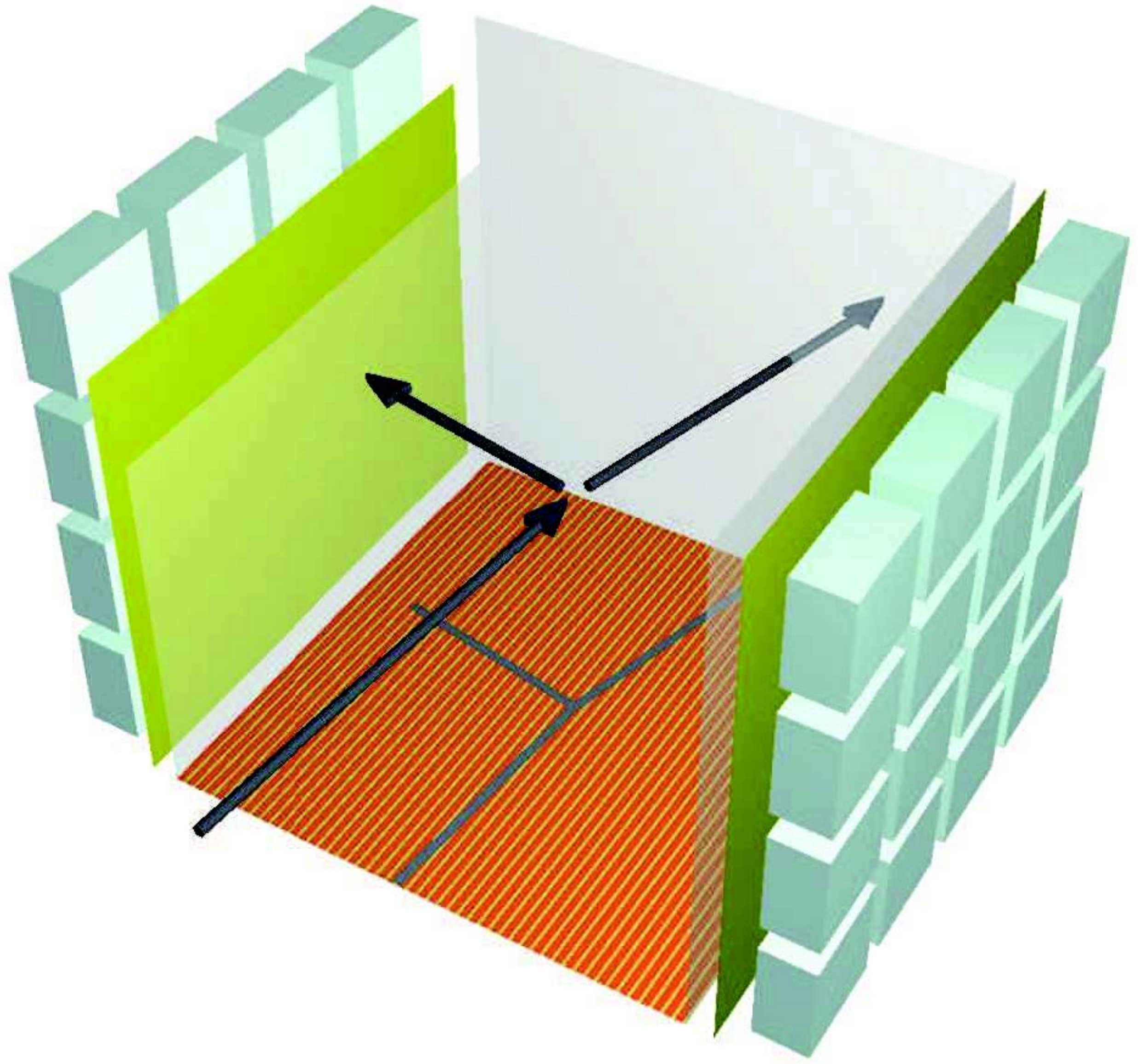

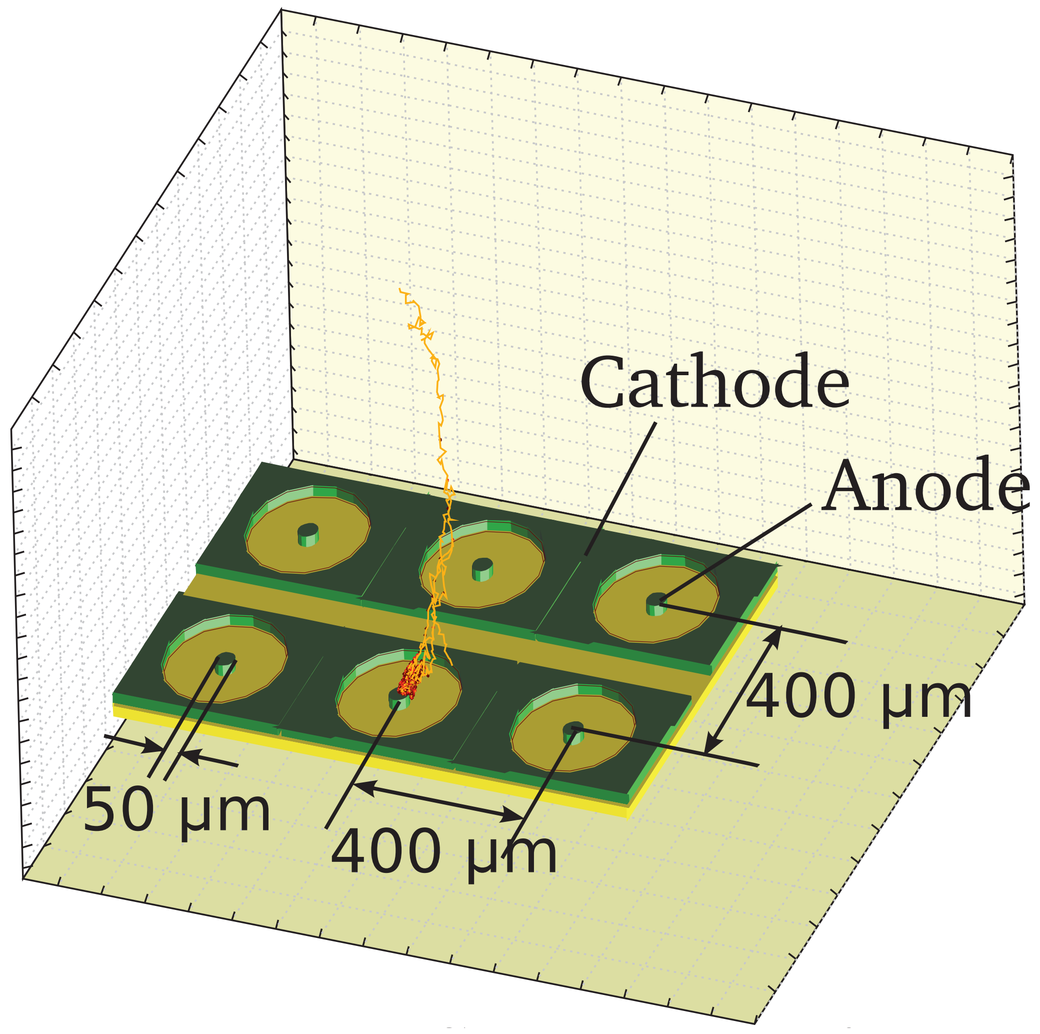

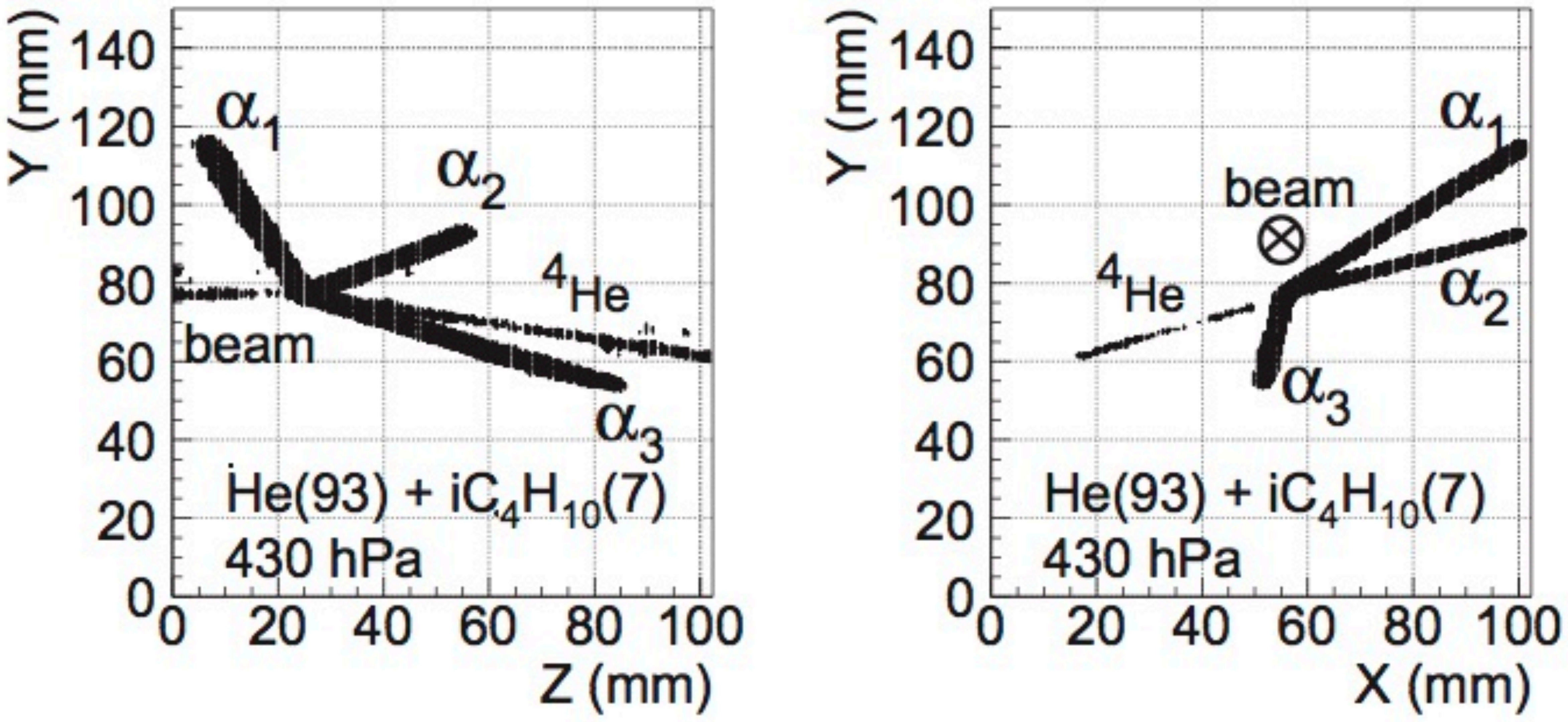

(a) anode (b) cathode

T. Furuno et al., Journal of Physics: Conference Series, Vol. 569, IOP Publishing, 2014, p. 012042

O-TPC in active mode

- $^{16}O(\gamma,\alpha)^{12}C$ photo-dissociation reaction HIγS beam
- 9.5 MeV γ-ray beam at 1.3 10^8 γ/s
- CCD camera records 2D projection of tracks
- Photo-multiplier records time evolution
- Energy loss profiles to identify ^{12}C and α
- Use of CO_2 (80%) + N_2 (20%) mixture
- Opens new possibilities to study photo-induced reactions at very low center-of-mass energies (astrophysics)
- Now possible to use pure CO_2 with THGEMs

M. Gai et al., JINST 5 P12004 (2010)

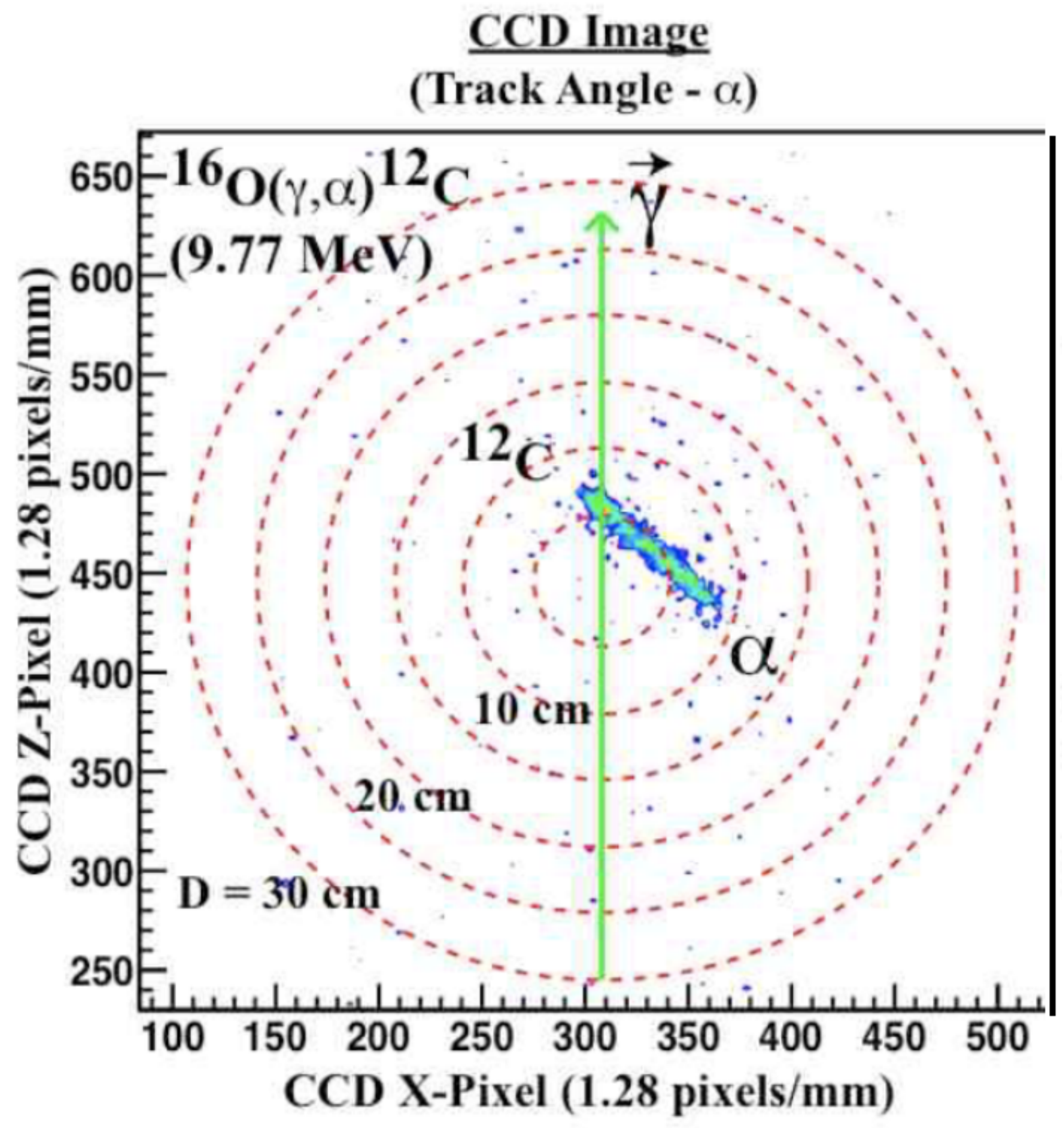

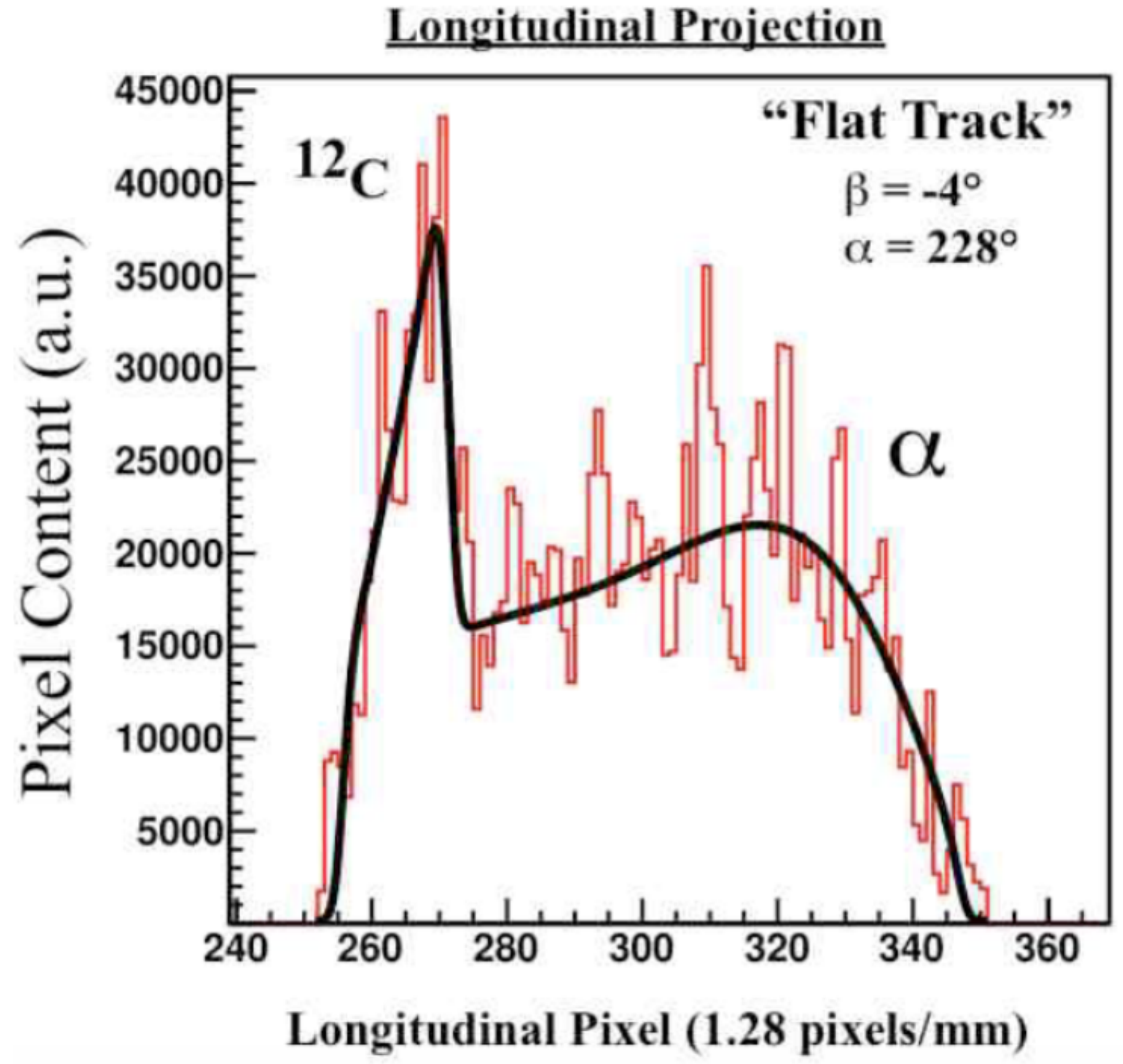

Prototype AT-TPC

- Half-size of full AT-TPC
- Proof-of-principle detector
- Designed for binary reactions
- Limited number of pads (253)
- Rings divided in 4 quadrants
- Trigger defined by coincidence between opposite quadrants

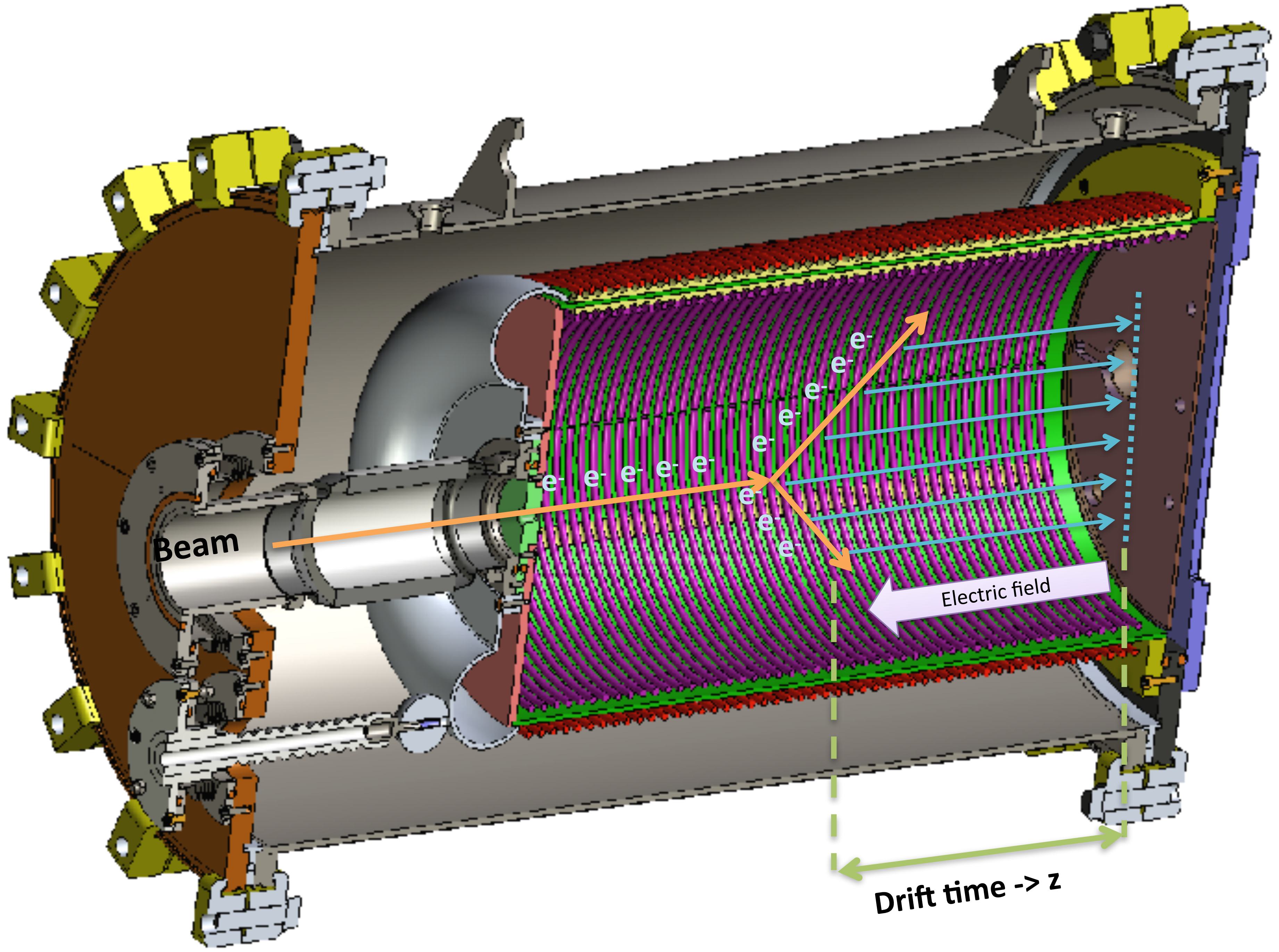

D. Suzuki et al., NIM A 691, 39 (2012)

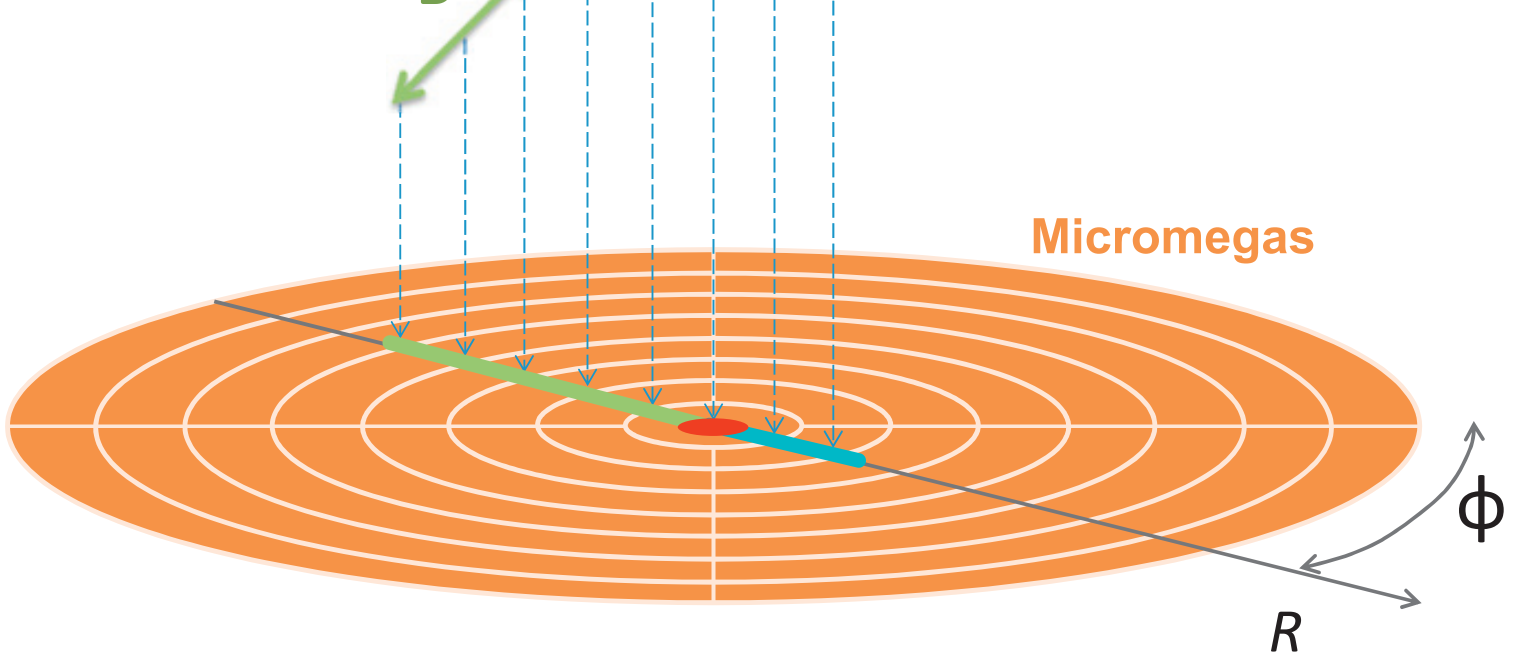

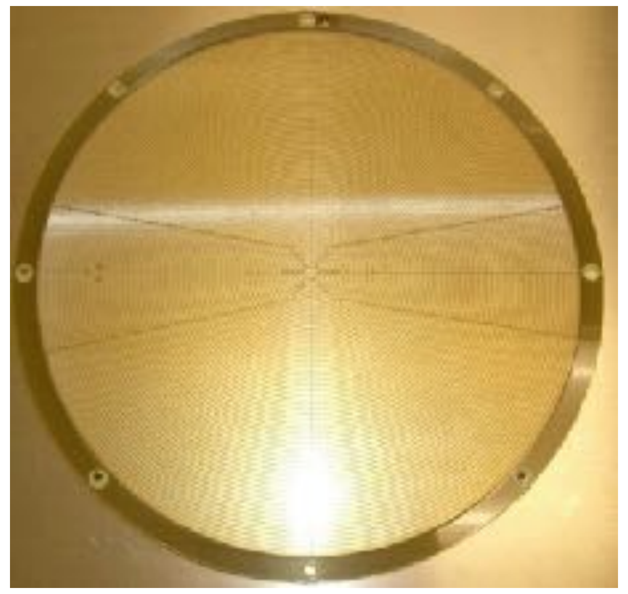

Alpha resonant scattering: ^{14}C

(pAT-TPC)

- ^{10}Be beam on He(90%)-CO_2(10%) gas
- Double-gain Micromegas to track both ^{10}Be and ^{4}He simultaneously
- Elastic and inelastic channels identified from kinematics
- Excitation function measured between 2-10 MeV (CM)
- Several resonances observed in both channels

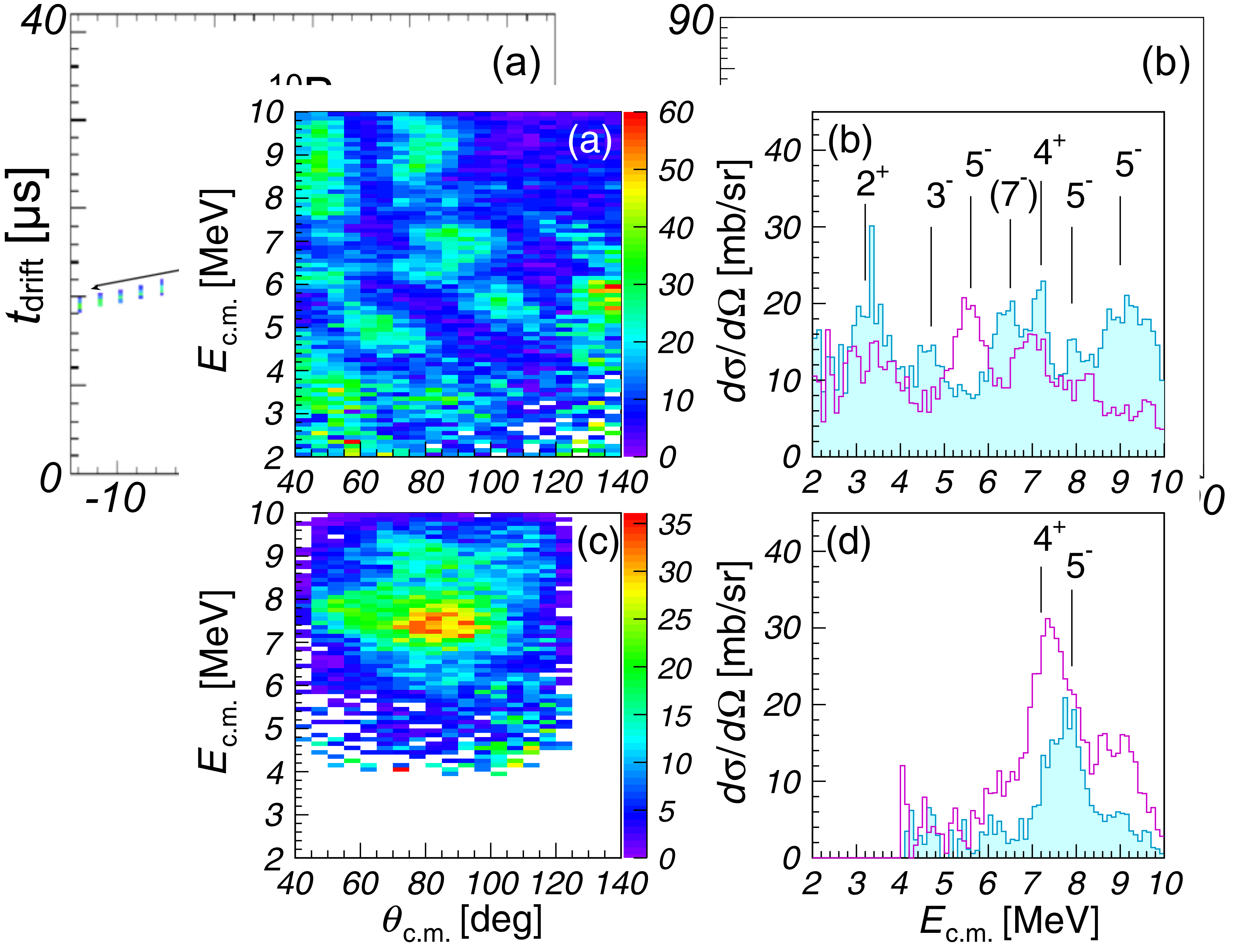

A. Fritsch et al., PRC 93, 014321 (2016)

Alpha cluster states in ^{14}C

- Resonances above $^{10}Be+^{4}He$ threshold
- 2^+ and 4^+ resonances clearly identified
- Compared with AMD calculations
- Linear chain looks most likely
- Finding 0^+ would confirm

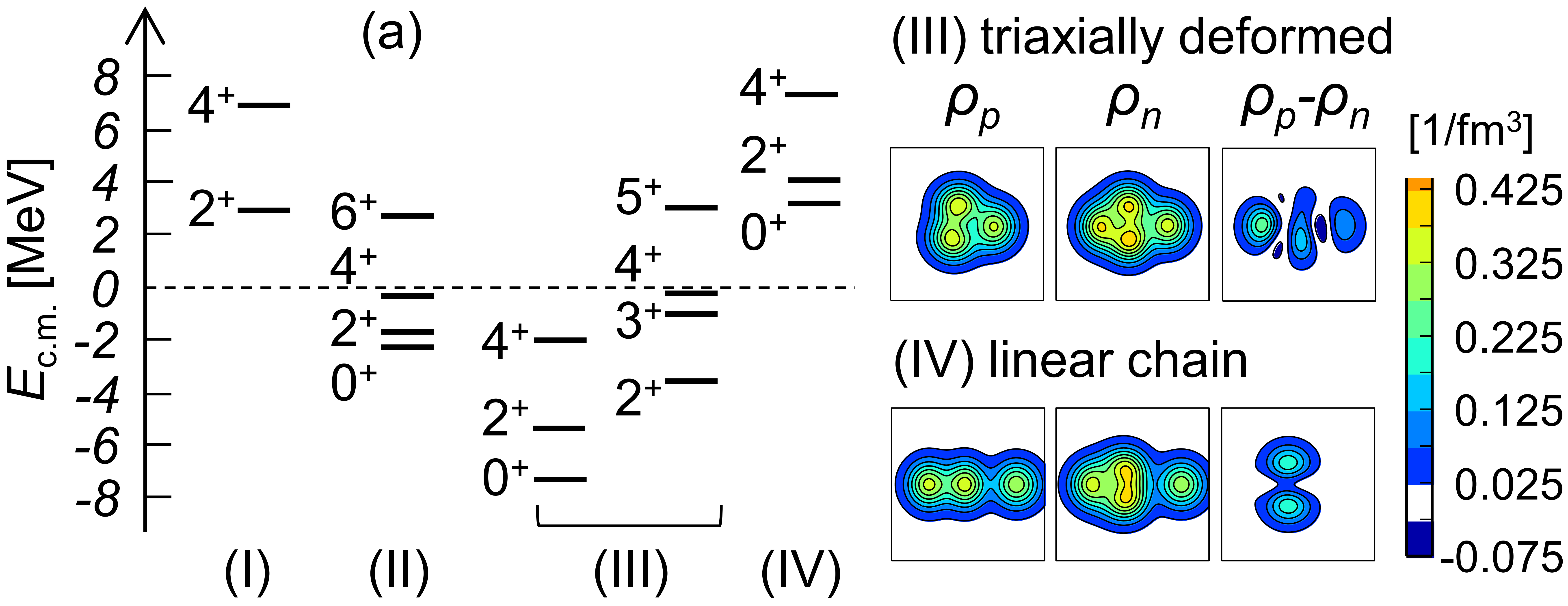

A. Fritsch et al., PRC 93, 014321 (2016)

Fusion cross sections

(pAT-TPC)

- ^{10}Be + ^{40}Ar fusion cross section
- Measured between 9-30 MeV (Lab)
- Fusion events identified using derivative of energy loss
- Excitation function of fusion cross section measured with 100 pps of beam only
- α-particle evaporation channel identified from energy loss profile

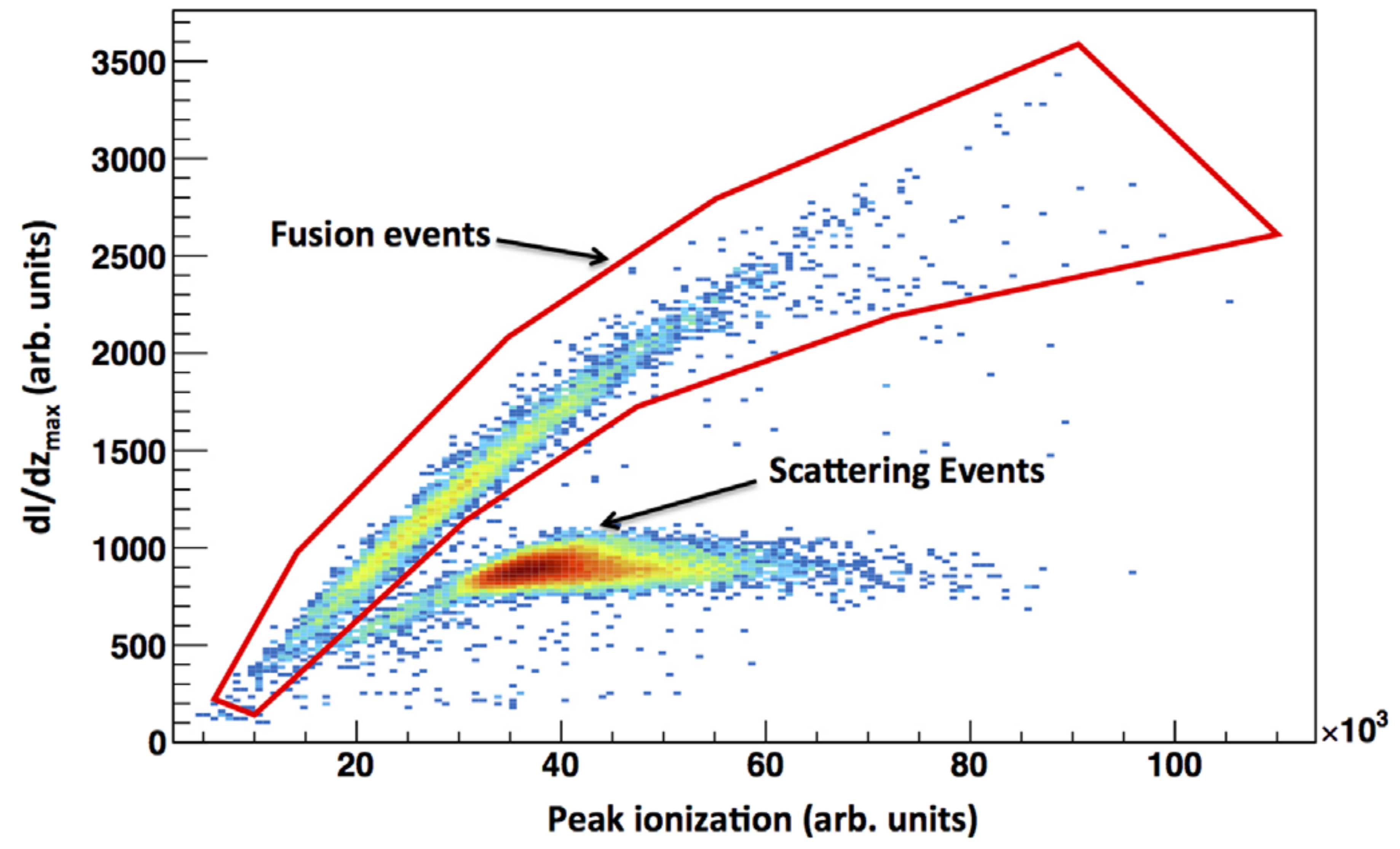

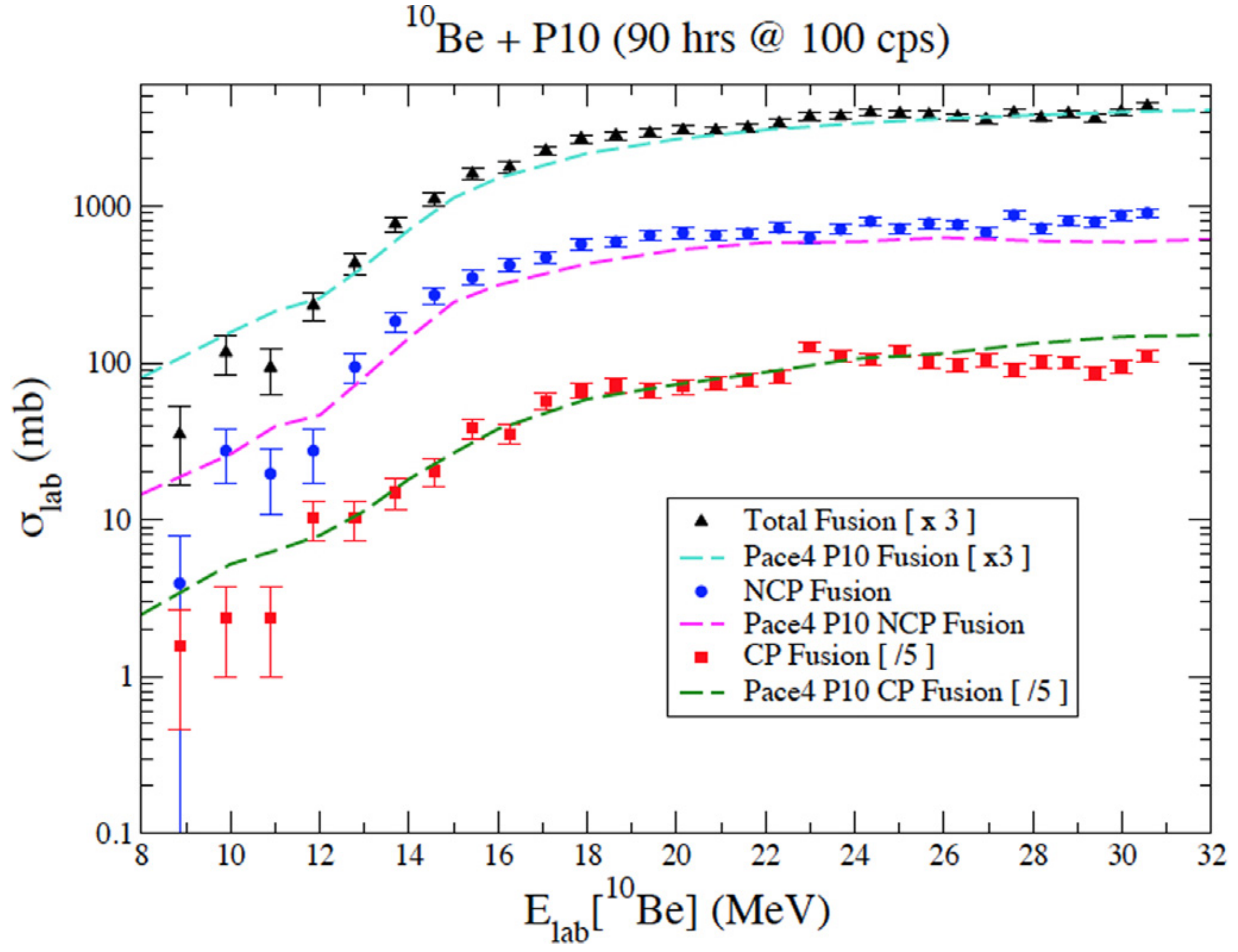

J. Kolata et al., NIMA 830 (2016) 82–87

^{11}Be β-delayed proton emission

(pAT-TPC)

- What? β-delayed proton from a neutron-rich nucleus?
  - Yes, because ^{11}Be is halo nucleus: quasi-free neutron decay into proton
  - Branching ratio could reveal neutron dark decay - related to neutron $T_{1/2}$ anomaly
  - But decay open by only 280 keV!
- Implant/decay experiment in pAT-TPC
  - ^{11}Be ions from ISAC (TRIUMF) implanted in He+CO2 gas
  - ^{11}Be half-life is 13.76 s: implant for 1 s, look at decays for 7 s

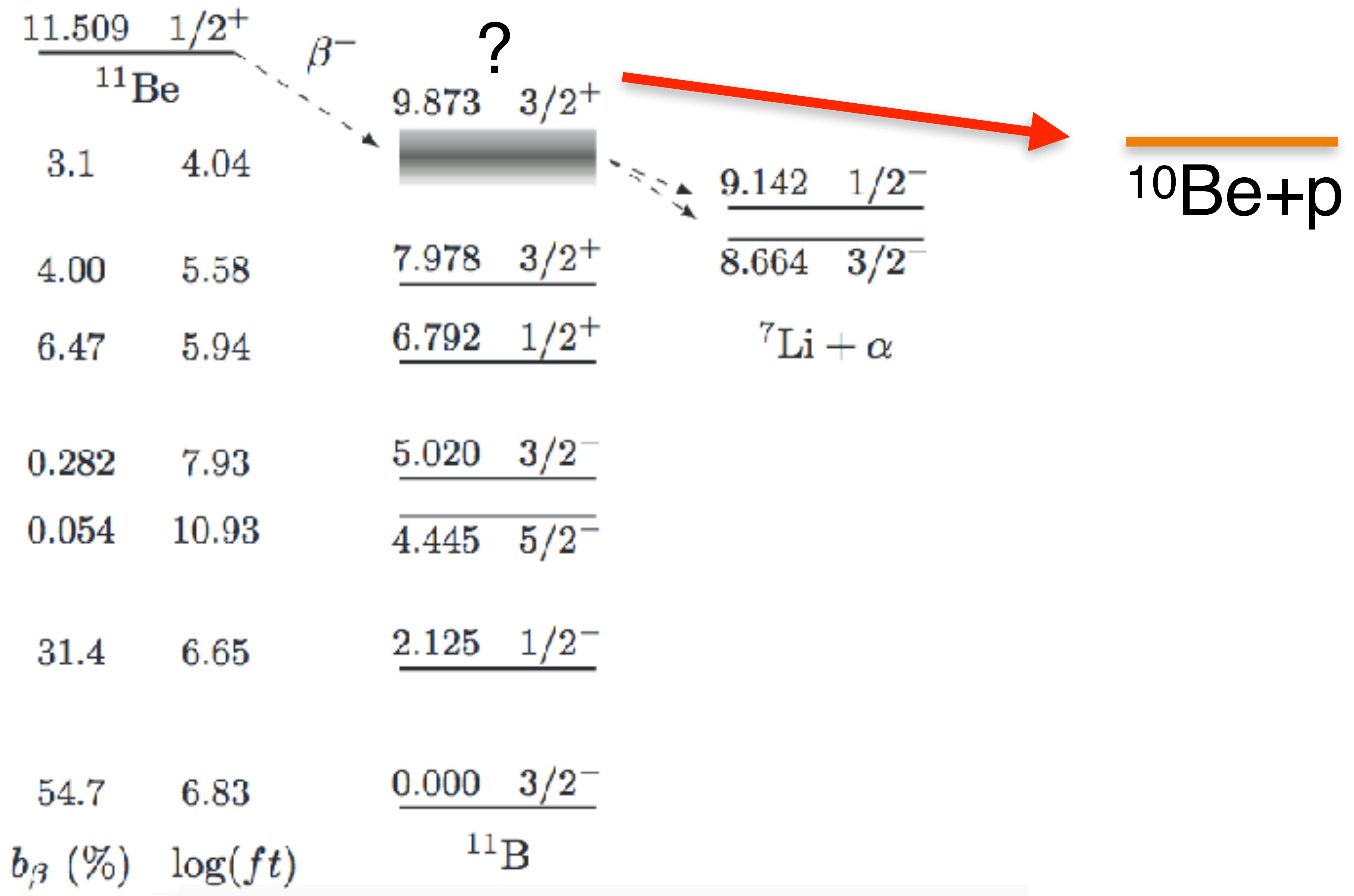

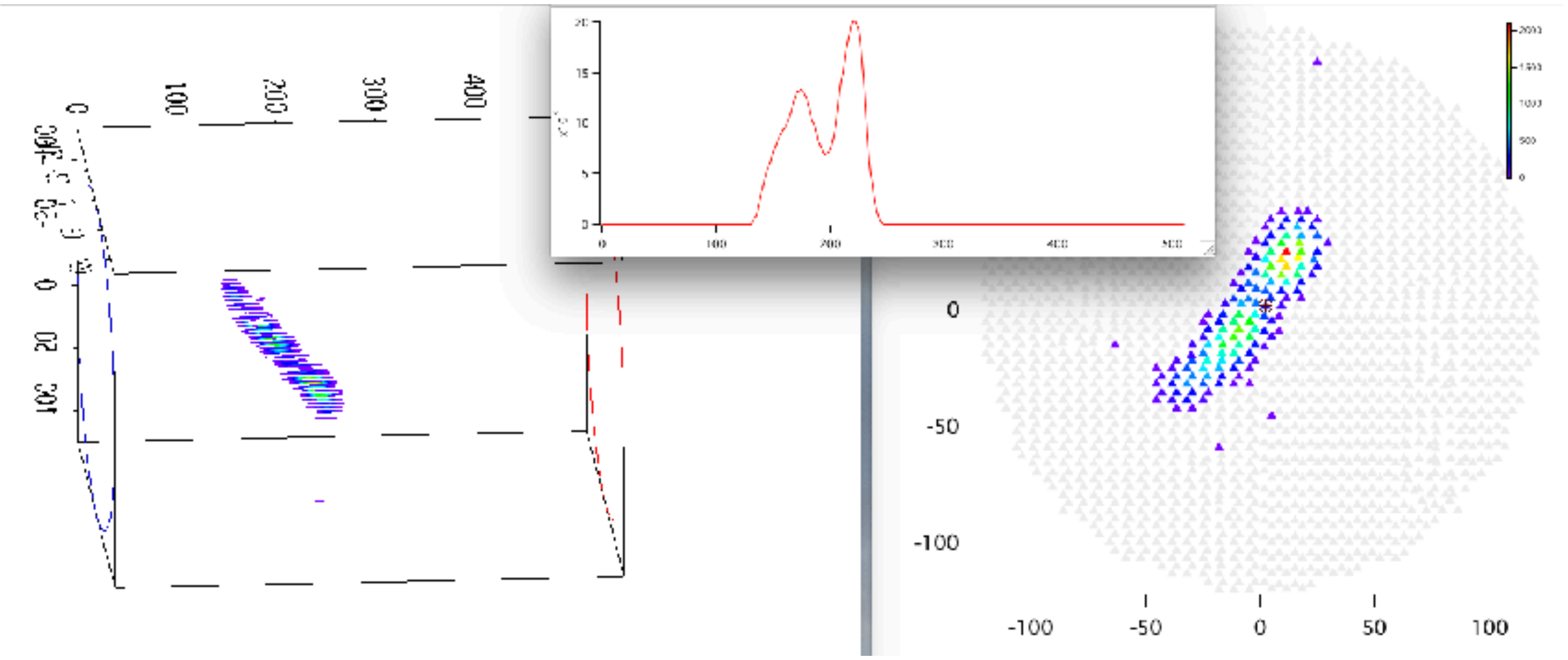

Identification of proton decay

- ^{7}Li energy similar to protons
  - Branch populating ^{7}Li*(1.2$^-$) gives ^{7}Li recoil < 300 keV
  - Calorimetry cannot separate them
  - 3% ^{7}Li+α branch orders of magnitude larger
- Energy loss profile
  - Significantly different between protons and ^{7}Li
  - X^2 analysis on energy loss profile below 300 keV allows identification of protons

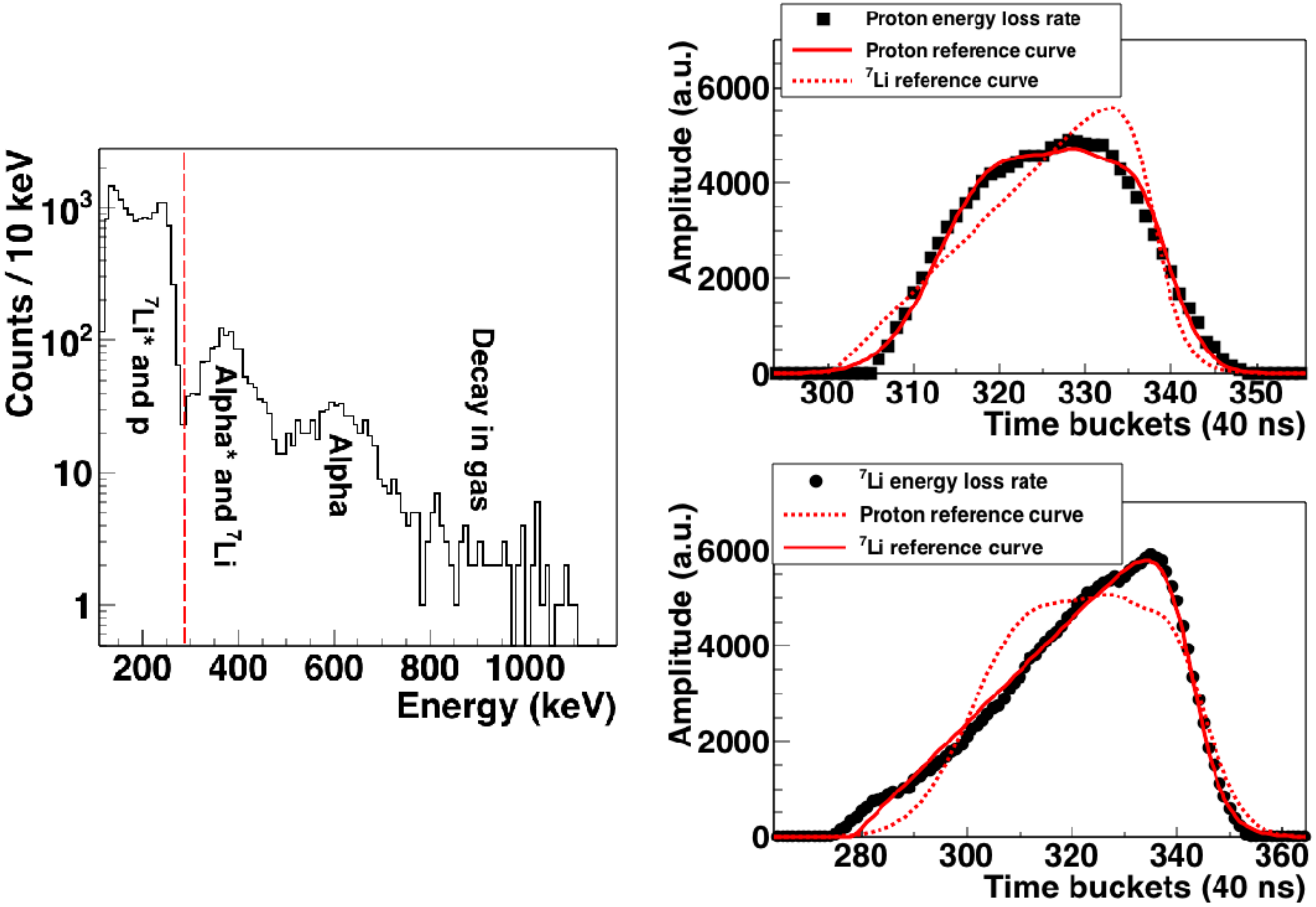

Results

- Direct observation of β-delayed proton emission from ^{11}Be
  - Measured branching ratio: 1.2×10^{-5} (30% error)
  - Accounts for all decays measured in CERN experiment
  - Sorry, no neutron dark decay involved
- Energy spectrum of protons
  - Hint of narrow resonance in ^{11}B at 11.425(20) MeV
- Next step
  - Use resonant proton scattering on ^{10}Be to find resonance in ^{11}B
  - Challenging experiment: ^{10}Be beam energy of ~ 300 keV/u and proton recoil down to 100 keV

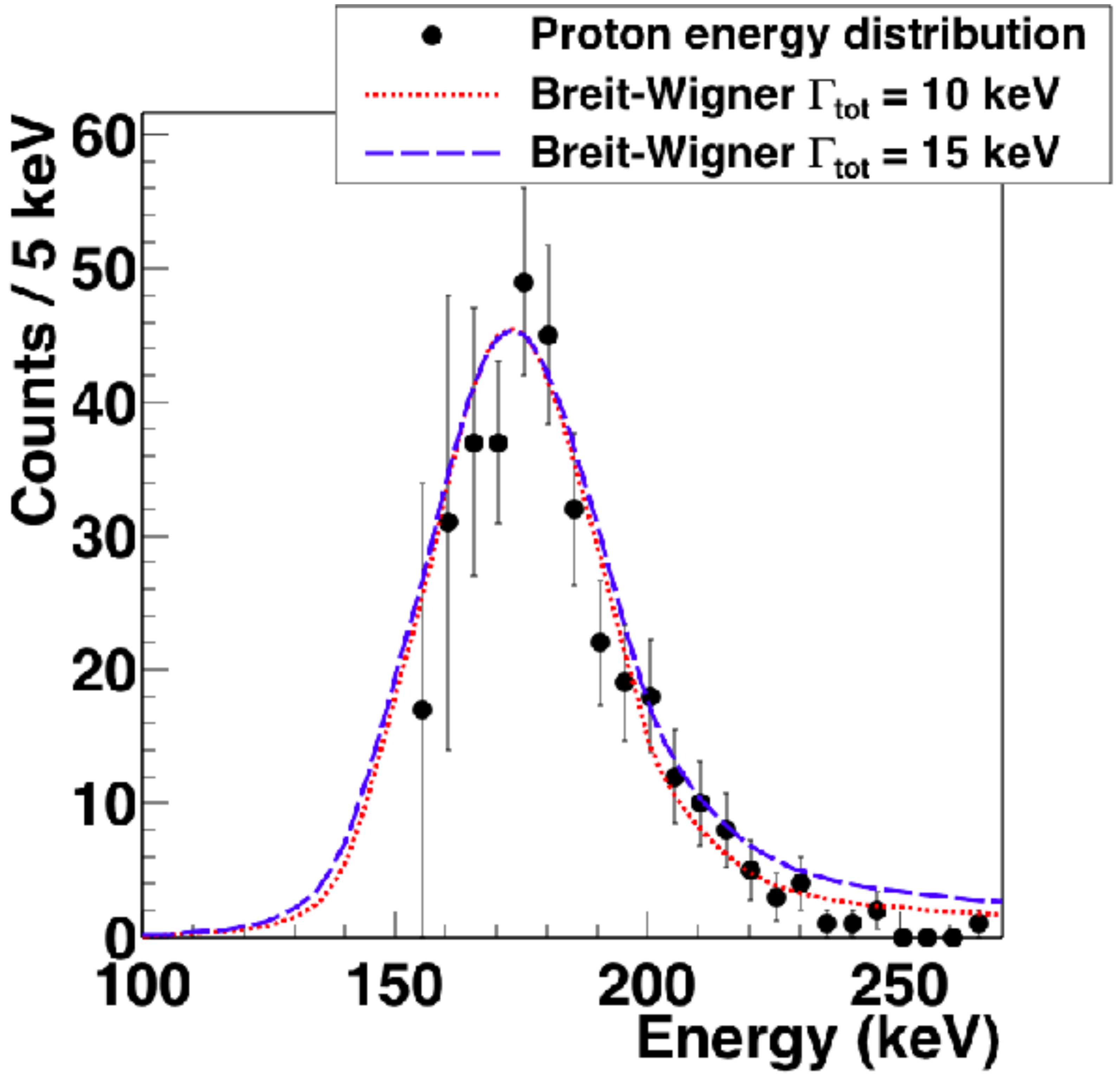

Y. Ayyad et al., PRL 123, 082501 (2019)

Resonant proton scattering on ^{46}Ar

- Proton scattering around the Coulomb barrier populate $T_<$ and $T_>$ states (resonances) of compound nucleus ^{47}K

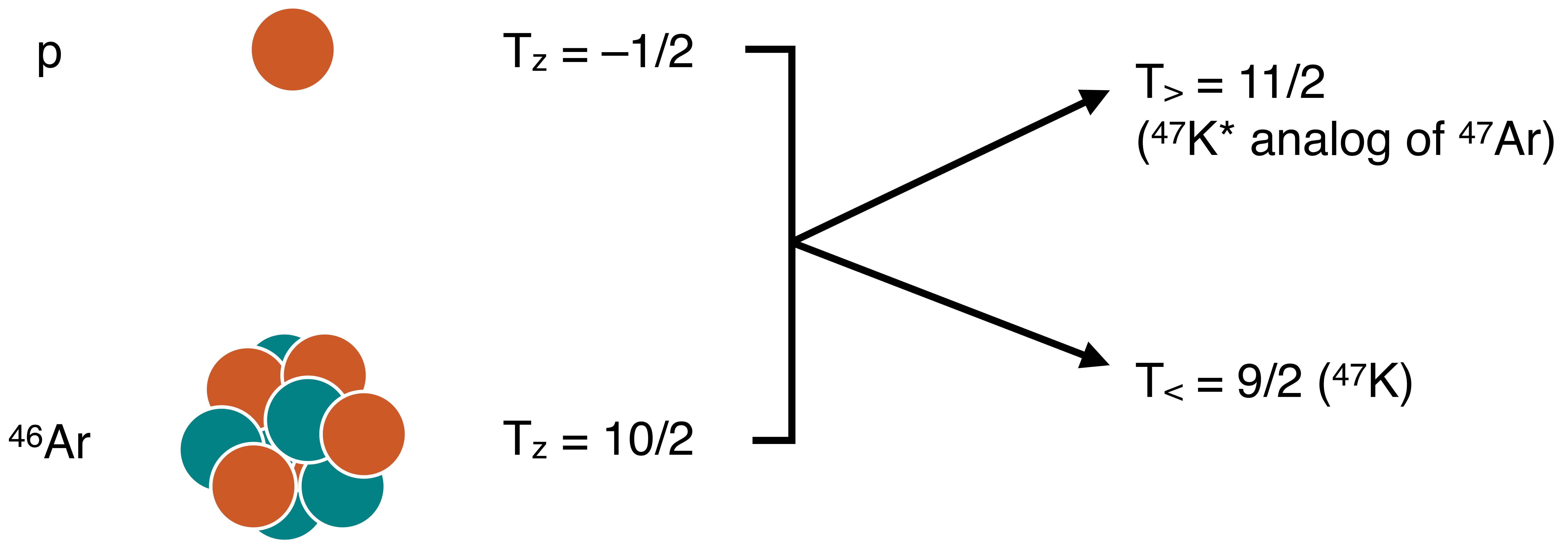

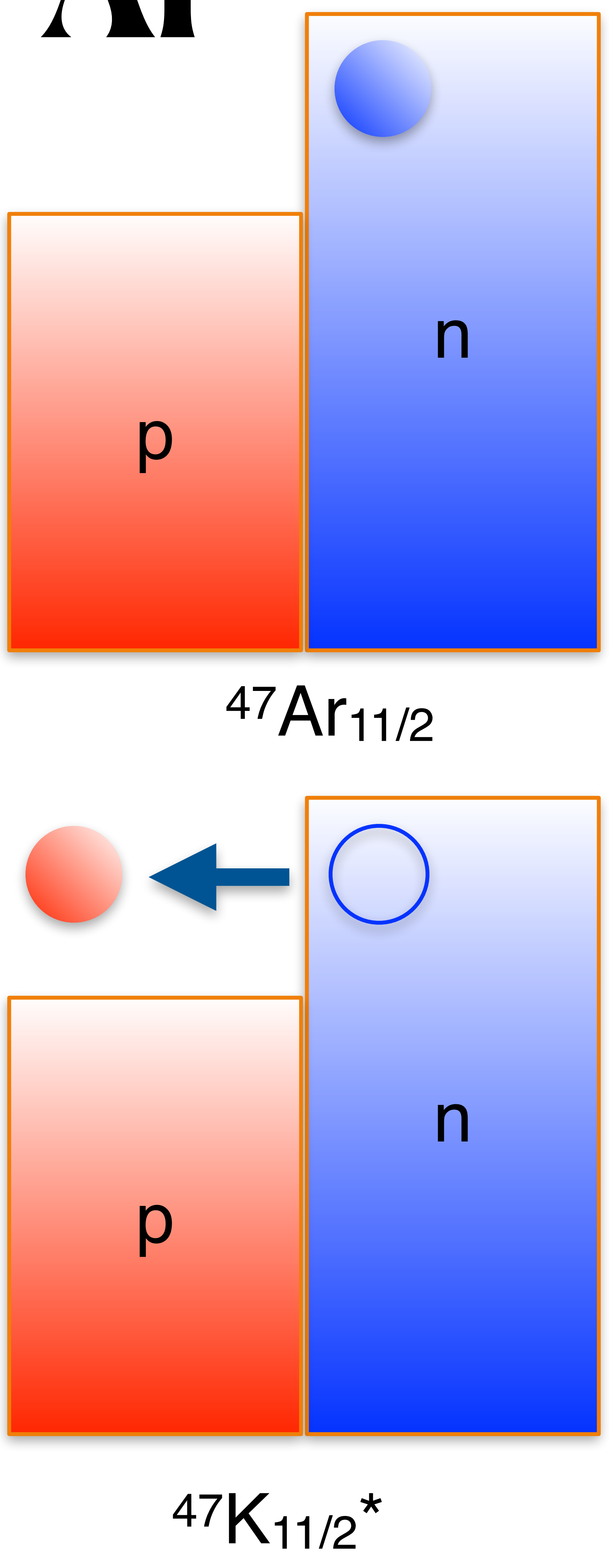

How to make a “nice” ^{46}Ar beam

- Commissioning run of full AT-TPC
- ^{46}Ar beam produced from fragmentation of 140 MeV/u ^{48}Ca
- Filtered by A1900 fragment separator
- Slowed down in thermalized in gas cell filled with ultra pure He
- Single-charge $^{46}Ar^{1+}$ extracted and stripped to $^{46}Ar^{17+}$ in electron beam charge breeder
- ^{46}Ar ions re-accelerated to 4.6 MeV/u by ReA3 linac

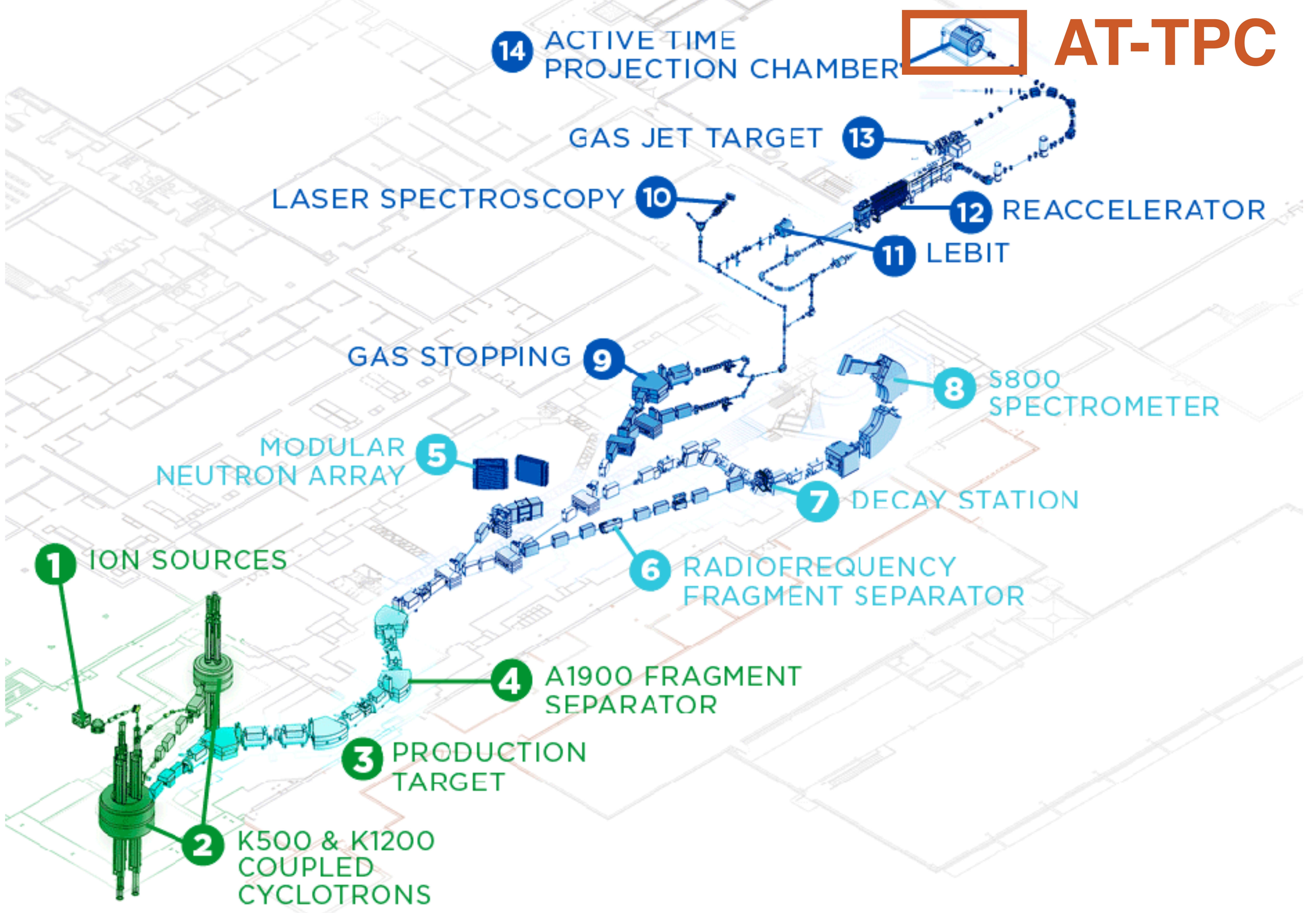

NSCL facility at MSU

See lectures from S. Liddick

Challenging analysis

- Several issues encountered
- Missing trigger module induced severe kinematical cuts
- Large ionization of ^{46}Ar ions compared to protons induced saturation on beam tracks and cross talk noise
- Low statistics due to use of C_4H_{10} instead of H_2
- Monte-Carlo fitting was the best method to extract physics (see Data analysis lecture)

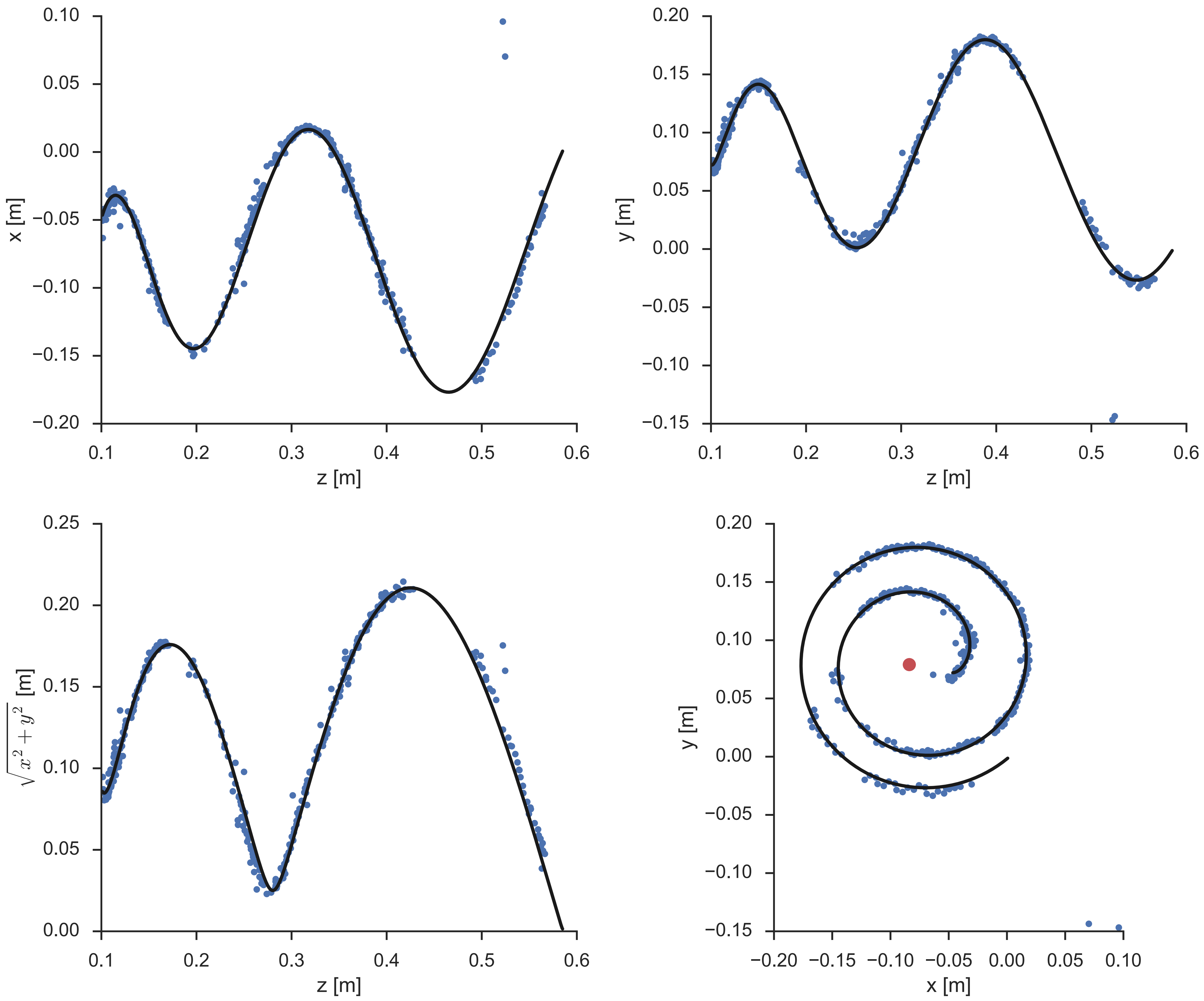

Results

- Fit using four resonances by adjusting energies, spectroscopic factors, widths in R-matrix calculation
- $T_>$ resonances in $^{47}K^*$ analog to $^{47}Ar_{gs}$ and $^{47}Ar_{1st}$, as well as possibly $T_<$ resonances
- Statistics is borderline

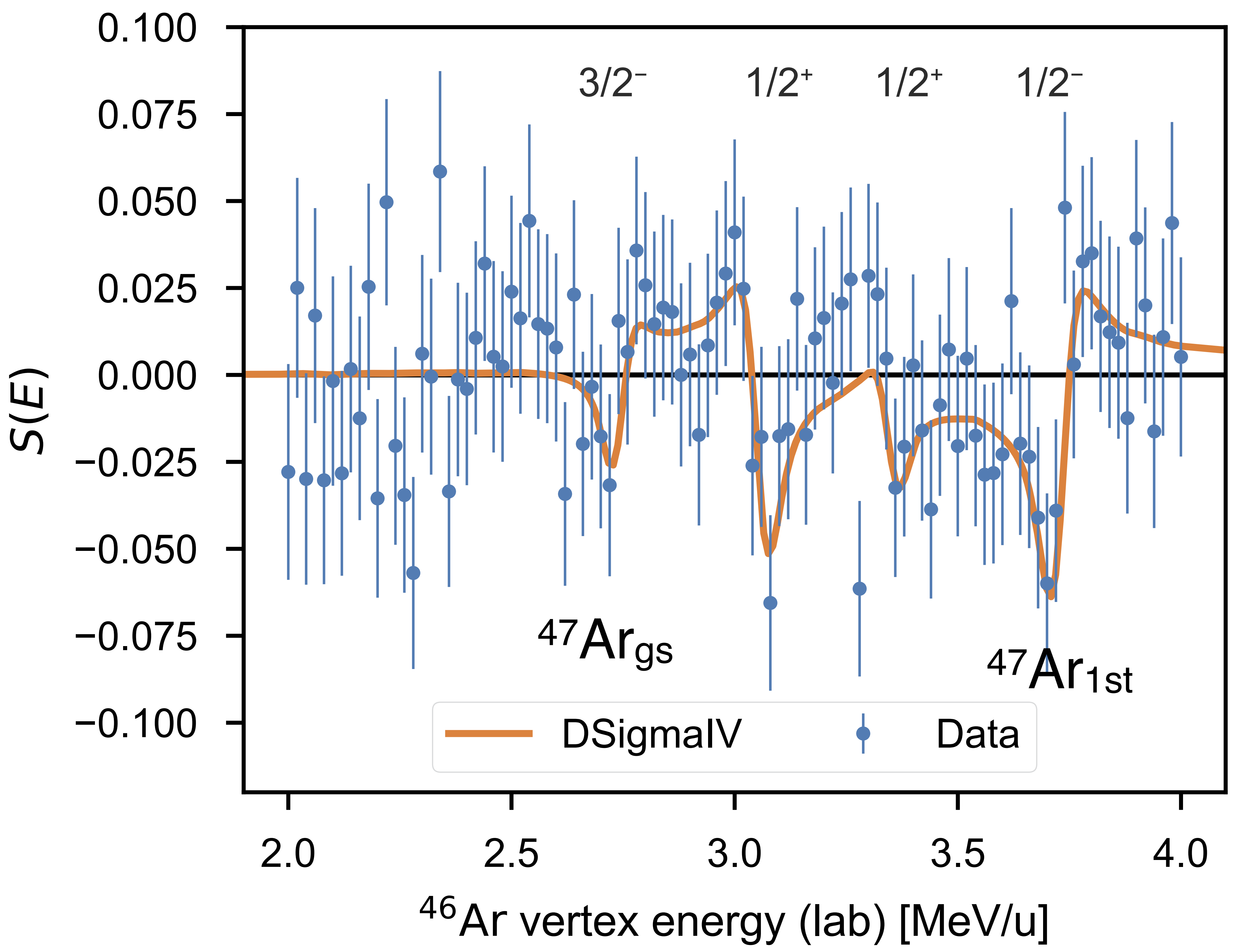

J. Bradt et al., Phys. Lett. B 778, 155 (2018).

$E_{\text{res}}^{\text{CM}}$ (keV)	E_x (keV)	J^π	T_z	S	Γ (keV)	Γ_p (keV)	F	p
$2680 \pm 108 \pm 20$	$0 \pm 91 \pm 28$	$3/2^-$	$11/2$ (^{47}Ar)	$0.27 \pm 0.03\ ^{+0.21}_{-0.13}$	15(10)	4.3(4)	2.14	0.15
$2990\ ^{+117}_{-124} \pm 20$	$310\ ^{+91}_{-92} \pm 28$	$1/2^+$	$9/2$ (^{47}K)	$0.027 \pm 0.006\ ^{+0.013}_{-0.007}$	30(10)	20(2)	3.59	0.04
$3280\ ^{+125}_{-127} \pm 20$	$600\ ^{+92}_{-93} \pm 28$	$1/2^+$	$9/2$ (^{47}K)	$0.008 \pm 0.002\ ^{+0.005}_{-0.006}$	18(10)	8.0(8)	0.68	0.58
$3650\ ^{+137}_{-147} \pm 20$	$970\ ^{+95}_{-99} \pm 28$	$1/2^-$	$11/2$ (^{47}Ar)	$0.42 \pm 0.05 \pm 0.09$	34(10)	24(2)	5.50	0.01

Resonant proton scattering with ACTAR

- ^{18}O 3.2 MeV/u beam on C_4H_{10} target
- Low electron gain region for beam
- High electron gain region for recoil
- Both (p,p) and (p,α) observed
- Kinematics resolution separate $^{18}O^*$
- Excitation functions show resonances in compound nucleus ^{19}F
- Very promising result for future radioactive beams!

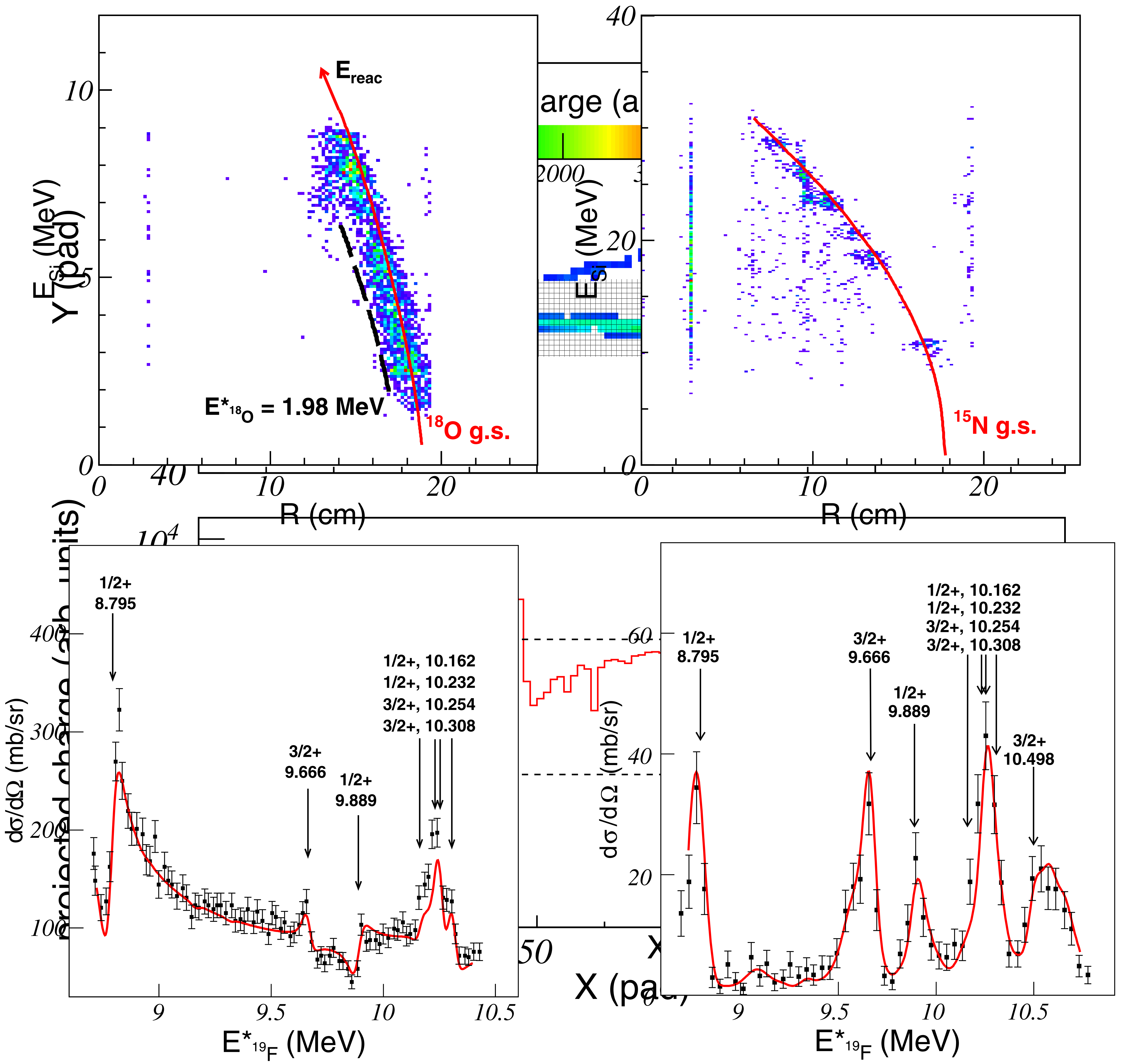

B. Mauss et al., NIMA 940, 498 (2019).

Astrophysical reaction $^{22}Mg(\alpha,p)^{25}Al$

- Important in type I X-ray burst burning
- ^{22}Mg re-accelerated beam at 5 MeV/u
- AT-TPC filled with He (95%) + CO_2 (5%)
- Signature of (α,p) reaction: single scattered proton track
- Several other types of events observed

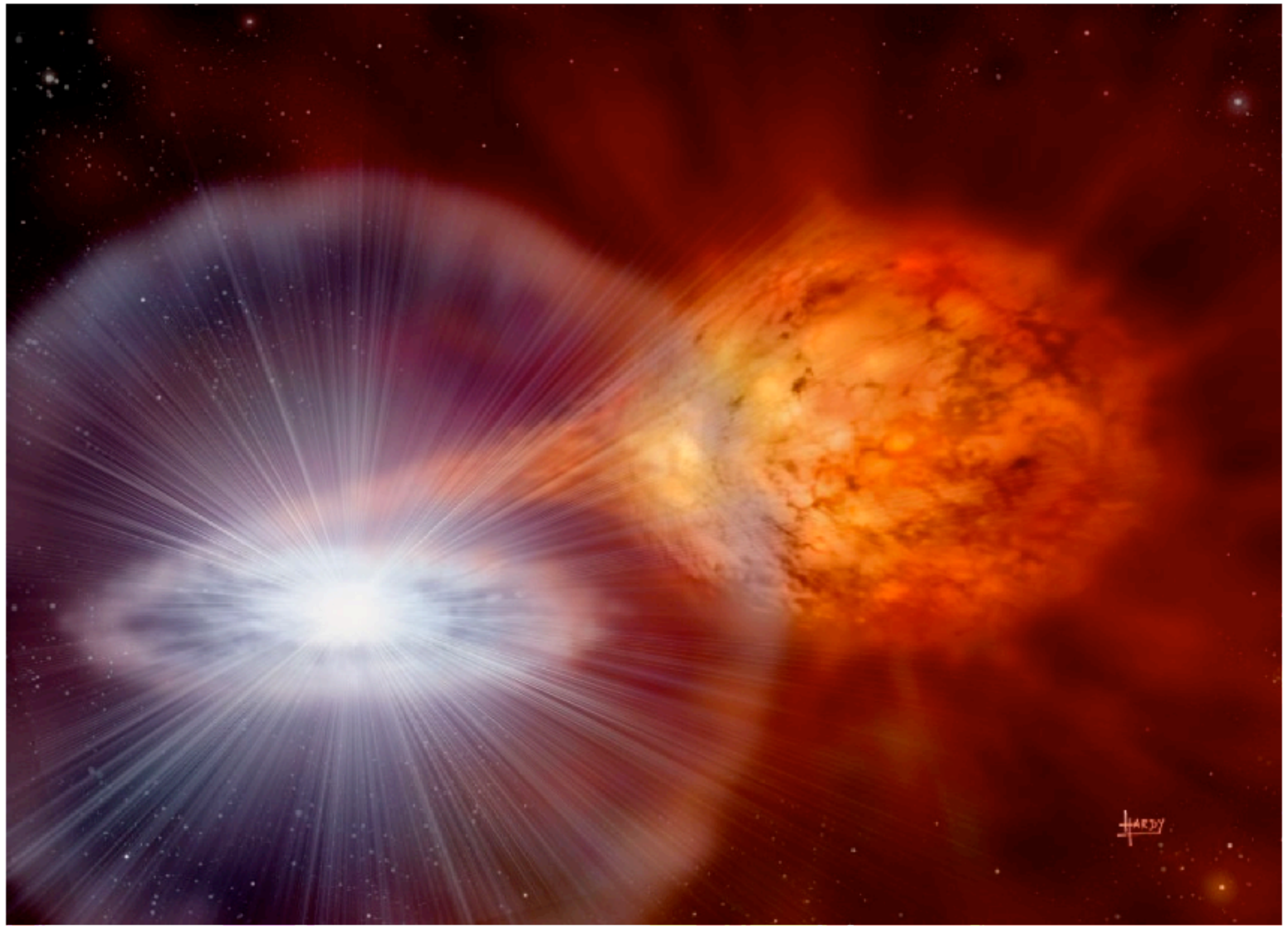

Gallery of events from ^{22}Mg experiment

^{22}Mg(α,α’)

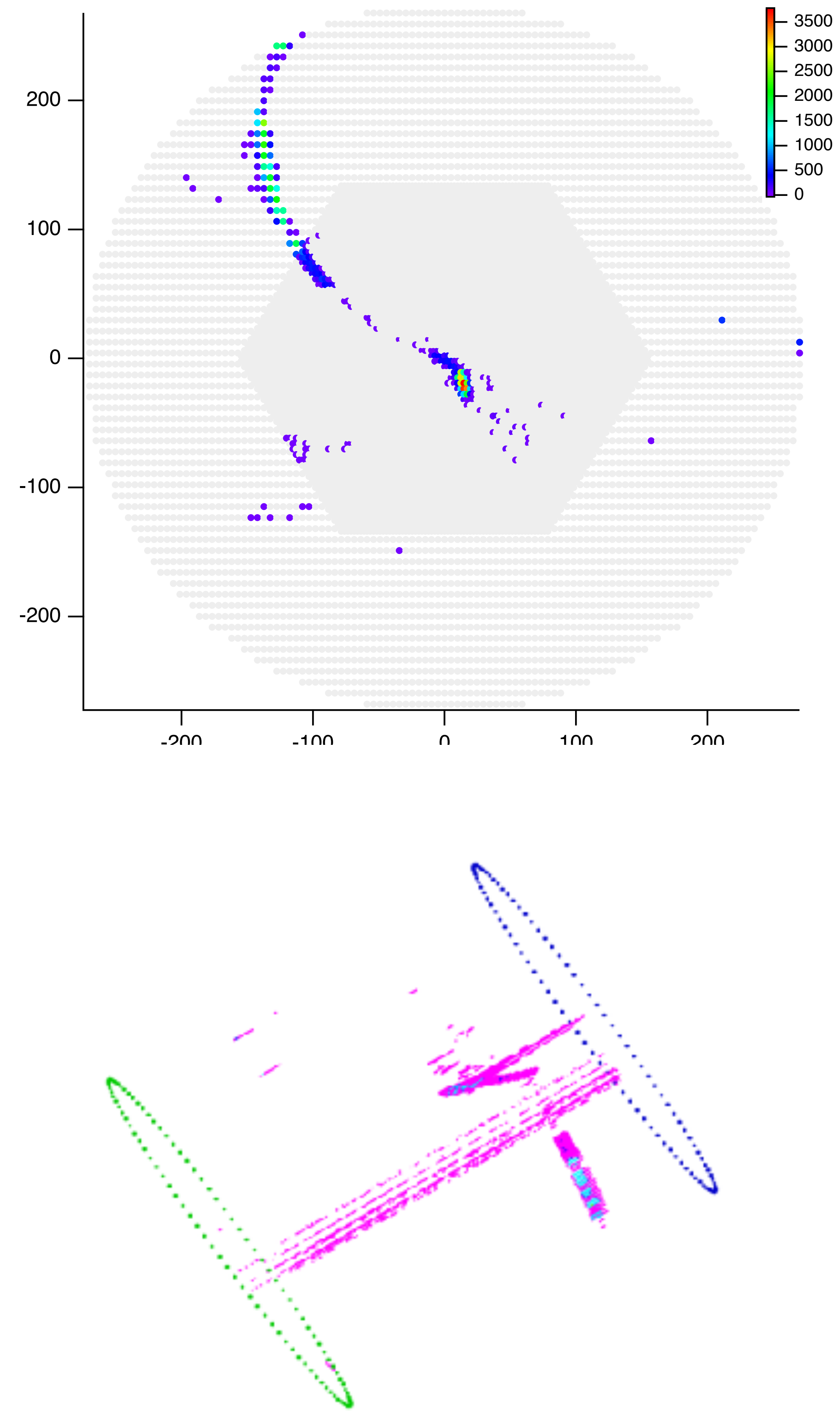

^{22}Mg(α,2p)

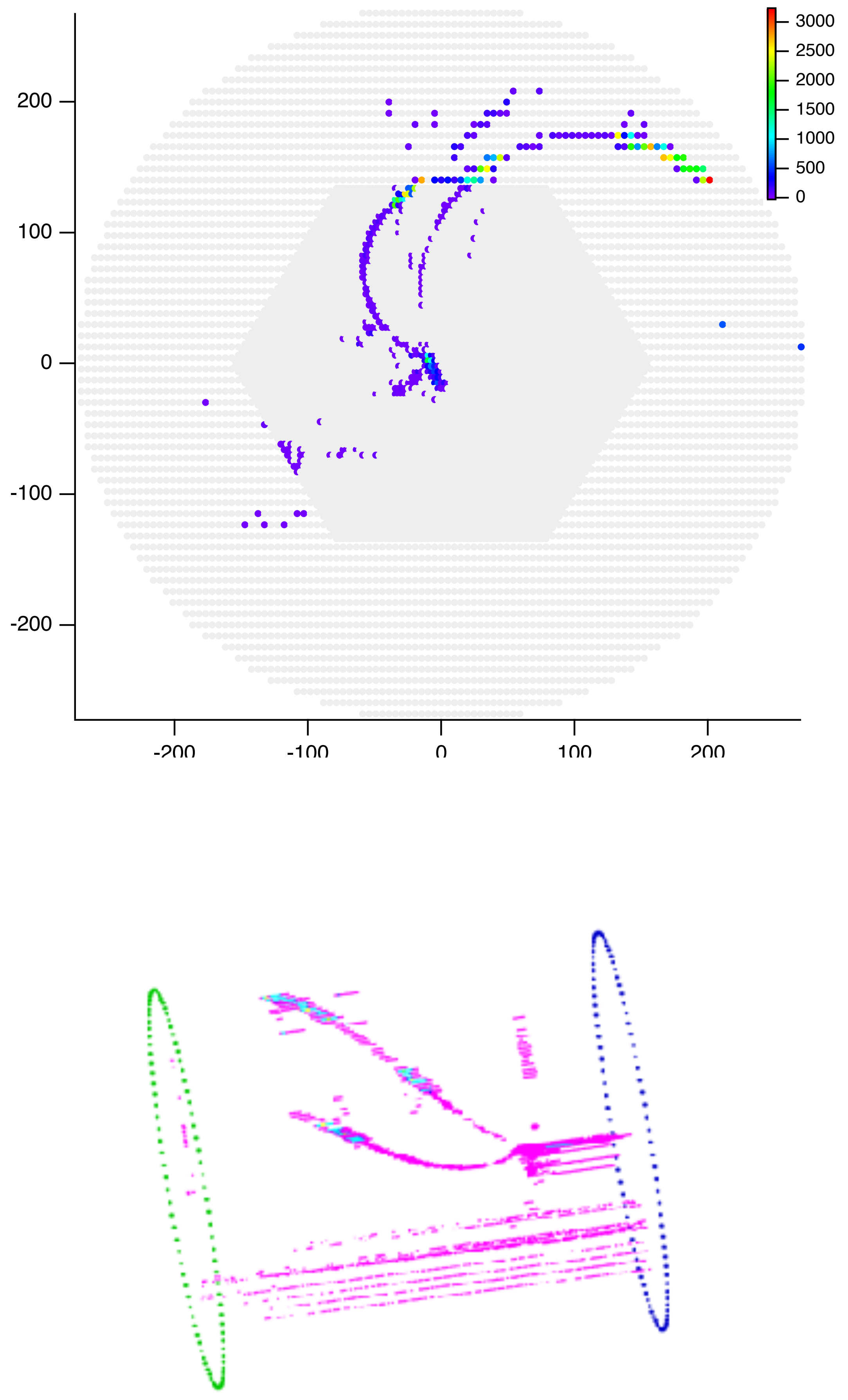

^{22}Mg(α,2pα’)

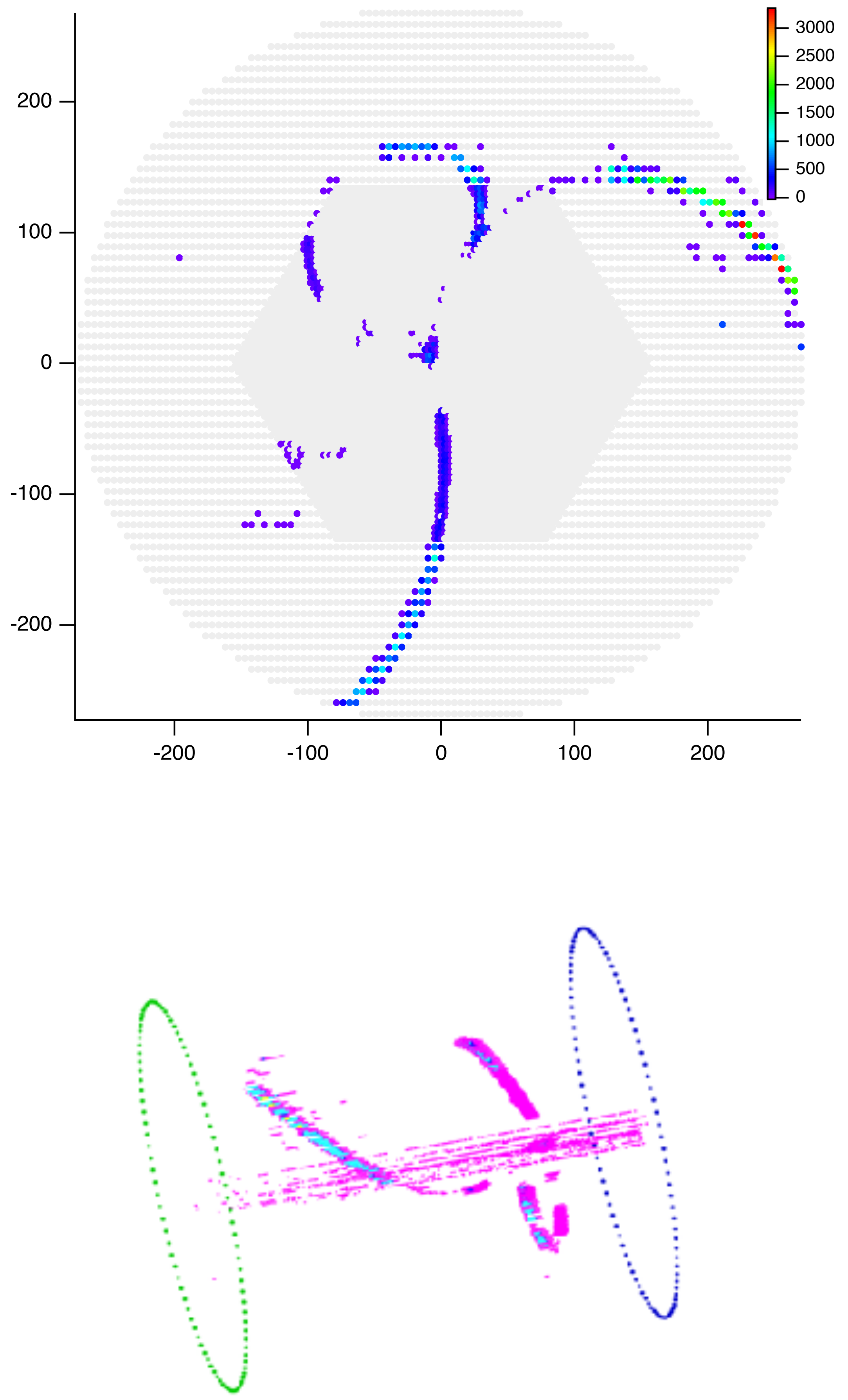

^{22}Mg(α,3p)

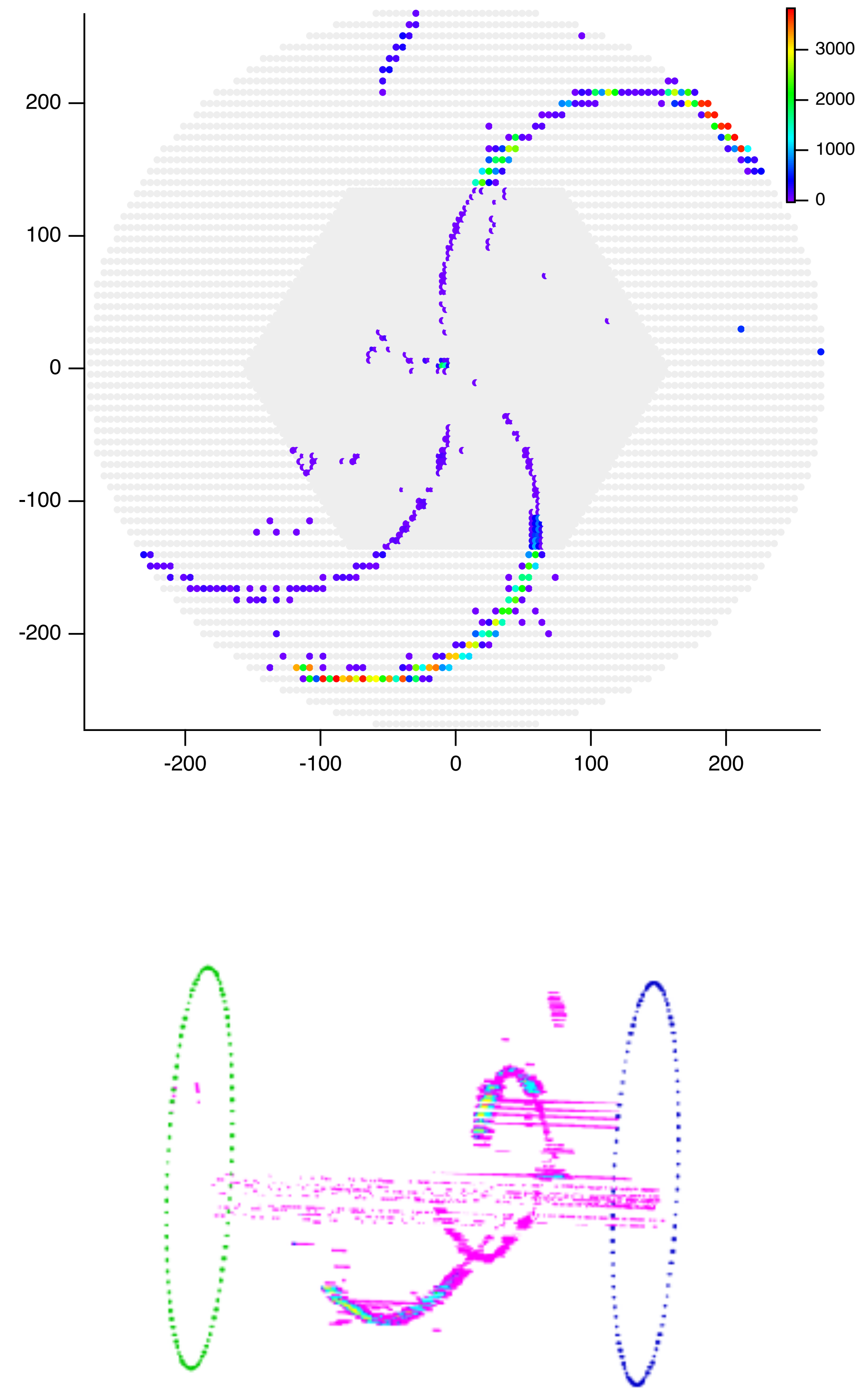

How do you find ^{22}Mg(α,p)?

D. Bazir

Concluding remarks

- Active targets are very versatile detectors
- Can be built to suit particular needs
- Boost luminosity of experiments using rare isotope beams
- Can cover several reaction channels
- Data analysis is challenging
- New methods are needed: Machine Learning!